THE UNIVERSITY OF MANITOBA

ON THERMAL CONTACT RESISTANCE OF COMPOUND CYLINDERS

by

W. K. Tam

A Thesis

Submitted to the Faculty of Graduate Studies

in Partial Fulfilment of the Requirements for the Degree

of Master of Science

Department of Mechanical Engineering

Winnipeg, Manitoba

March, 1976

"ON THERMAL CONTACT RESISTANCE OF COMPOUND CYLINDERS"

by

W. K. Tam

A dissertation submitted to the Faculty of Graduate Studies of the University of Manitoba in partial fulfillment of the requirements of the degree of

MASTER OF SCIENCE

ABSTRACT

Previous investigators have extensively studied the problem of interface resistance for two plane surfaces in contact from a variety of points of view. An attempt is made in the present investigation to study the thermal contact resistance of an aluminum-stainless steel compound cylinder. Because no other work of this type has been done, two plane-contact interface models - Shlykov and Ganin model and Modified Ross and Stoute model were employed to compare with the measurements. Experimental evidence showed that the thermal contact resistance for a cylindrical interface is lower than that for the plane-contact interface. Physical interface models which explain the phenomenon are presented.

ACKNOWLEDGEMENTS

The author wishes to express his sincere appreciation to his advisor, Dr. T. R. Hsu, for his continuing assistance, advice, and guidance. Also, appreciation is gratefully given to Mr. G. Bertels for his valuable suggestions and advice in the experimental work.

The author would like to take this opportunity to thank Mr. L. W. Wilkins, Mr. R. Sharpe, and Mr. F. Christian for their assistance during the preparation of the test apparatus. Thanks are also due to Dr. K. K. Tangri for the permission to use the spark-erosion machine and to the staff of the Metallurgy Group in the Mechanical Engineering Department for their assistance in preparing the test specimens. My thanks also goes to Ms. Burga Kruse for typing the thesis.

The financial support provided by the National Research Council of Canada is also acknowledged.

Above all, the author would like thank his wife, Jane, for her patience and encouragement during the course of the study.

TABLES

LIST OF FIGURES

NOMENCLATURE

a	radius of contact
a_o	constant having dimensions (length)
A_α	apparent contact area
C	coefficient
E	modulus of elasticity
H	microhardness
k_M	harmonic mean thermal conductivity of metal
k_1 and k_2	thermal conductivity of aluminum and stainless steel respectively
k_F	thermal conductivity of interfacial medium
P	pressure
P_c	contact pressure
P_i and P_o	internal and external pressure respectively
P_{sc}	contact pressure due to shrink fit
P_{tc}	contact pressure due to thermal loading
Q	rate of heat flow
R_c	thermal contact resistance
R_F	thermal resistance of interfacial medium
R_M	thermal resistance of direct metal contact
r_1, r_2 and r_3	inside, interface and outside radius of compound cylinder respectively
T	temperature
T_c	interface temperature
u	radial displacement
ΔT_c	interface temperature drop

α	coefficient of thermal expansion
ν	Poisson's ratio
δ	interference of metal
σ	RMS roughness
σ_B	ultimate strength
σ_{rr}, $\sigma_{\theta\theta}$ and σ_{zz}	stress components of composite cylinder in cylindrical coordinate

CHAPTER 1

INTRODUCTION

Present day heat transfer problems between metallic members in contact are currently of great interest. This recent surge of interest arises mainly in connection with the thermal design of space vehicles and nuclear reactor fuel elements.

The simple analysis of this problem is based on the assumption that the surfaces of the contacting bodies are in perfect contact, in other words the thermal contact resistance is zero, and this has been used in many engineering problems. It simplifies the problem and to a certain extent does not seriously affect the results. But for certain applications where high accuracy and precise calculations are required, such an idealization can lead to a considerable error in the predicted performance.

One typical application which gives occasion to the study is the thermal contact resistance between the fuel pellets and its surrounding sheath in a nuclear reactor. Because of high intensity of heat flows passing through the fuel pellets to its sheath, the thermal contact resistance due to the absence of close contact will greatly affect the heat transfer conditions between the solids. Furthermore, as in the design of space vehicles, thermal contact resistance appears to be a critical design factor in attaining a high reliability for vehicle temperature control. Thus, an accurate knowledge of the thermal contact resistance between metals is indeed vital.

1.1 Definition of thermal contact resistance.

When two solid surfaces are brought into contact, because of the nature of the surface of any material, actual physical contact only

takes place at a finite number of discrete points. The actual contact area is only a small portion of the nominal contact surface, and this is true even with very high compressing forces and high quality of surface finish. There remains the voids which usually filled with fluid. While heat is flowing through the contact members, an additional temperature drop which is associated with the thermal contact resistance will occur at the interface of the joint.

The thermal contact resistance is not only a thermal effect, but also coupled with the surface characteristics and mechanical effect (surface deformation). The mode of heat transfer by which heat transported through the interface may, in general, be considered as follows:

1. by heat conduction at the points of direct contact (metal and/or oxide contact);
2. by heat conduction through the fluid filling the void;
3. by radiation between the metallic surfaces;
4. by natural convection in the fluid filling the void.

In most cases, both the natural convection and radiation in the void are neglected as the voids are usually very small and the interface temperature is not high. However the radiation effect may become significant and must be taken into account at high temperatures. Heat conduction through the places of direct contact and interfacial fluid is, therefore, considered to be the main cause of the thermal contact resistance in common place.

The thermal contact resistance is conventionally defined as:

$$R_c = \frac{\Delta T_c}{Q/A_\alpha} \tag{1}$$

where ΔT_c is the temperature drop at the interface, Q the heat flow rate across the contact, and A_α the apparent contact area.

It is understood that the thermal contact resistance is the reciprocal of thermal contact conductance. Thus, whenever thermal contact conductance is referred to, thermal contact resistance is implied. Through out this work, the thermal contact resistance concept will be used.

1.2 Literature survey.

In the past thirty years considerable effort has been expended to investigate the problems related to thermal contact resistance. A comprehensive review of the literature in this field was provided by Clausing and Chao [1]. Experimental and theoretical work were carried out in an endeavor to understand the nature of the thermal contact resistance from a variety points of view.

Jacobs and Starr [2] conducted experiments on interface joints between gold, silver and copper. Studies of contact resistance on machine joints were reported by Weills and Ryder [3], and Brunot and Buckland [4]. Barzelay et. al. [5,6] presented a comprehensive investigation on the effect of surface condition, interface temperature, interface pressure, heat flux and sandwich material on thermal contact resistance. Theoretical formulations are given by Fenech and Rohsenow [7], Laming [8] and Sanokawa [9,10], but they are all of limited values as the effect of the surface deformation and the non-uniform conditions over the contact surface were not taken into account in their analysis. Motivated by Barzelay's result, several notable works on the directional effect

are reported. Clausing [11] showed that the thermal strain can be the source of the directional effect. An extension of this particular field by Lewis and Perkins [12] revealed that the pronounced effect is strongly dependent on the contact surface condition. Loading hysteresis effect was analytically studied by Mikic [13] and Popov [14], and was found to be significant. With experimental evidence, Popov [14] showed that the thermal contact resistance for initial loading is higher than that for subsequent loading. In reference [15] the effect of plating with materials of higher conductivity than the plated material was treated and the results indicate that a considerable reduction in contact resistance can generally be obtained.

Surface characteristics are well recognized to be a striking factor in determining the thermal contact resistance. Interest in the area of surface description (i.e. waviness and roughness) and surface behavior (i.e. mode of deformation) arose in the mid-1950s due to the need for more accurate predictions, especially for the thermal design of nuclear reactors. References [16] to [27] are some of the most salient literatures in this area. In particular, Mikic [26] gave an elaborate report on the effect of mode of deformation on contact resistance, and criteria were also presented to determine the mode of deformation. Others [7-13] on the surface description under given mode of deformation (usually plastic deformation).

A theoretical investigation on the influence of the material anisotropy was carried out by Vutz (27). A geometric transformation technique was used in the analysis, and it was found that the degree

of anisotropy and orientation of the contact interface can be important factors.

In 1971, Yovanovich performed a theoretical and experimental study on the thermal contact conductance of turned surfaces (28) and a row of cylinders contacting two planes (29) which is of direct interest to aerospace engineers. More recently several significant works (30, 31,32) were published in an effort of seeking a better explanation and accurate estimation of the contact resistance.

1.3 Objectives of this work

A review of the open literature indicates that all the previous investigations laid the emphasis on the plane contact surface. No work has been done on any other interface configuration until recently (29, 31). The conventional idealized model used by all the previous investigators is a right circular cylindrical heat channel, and the general experimental installation is of two cylindrical models pressed together with heat flowing in the longitudinal direction. The interface for these models is a plane surface. It was suggested that the conventional analysis and experimental results, to some extent, can be applied to other shapes of contact surface.

Yovanovich proposed [33],

> .... other shapes of heat flux tube can arise which are but modifications of the one which we shall use. As examples, consider the contact between concentric pipes or concentric spheres,...

Cooper et. al. suggested (24),

> .... in terms of flow of heat through large plane interfaces can reasonable be extended, with obvious verbal changes, to apply to curved surfaces such as concentric cylinders with radial heat flow, provided the radius of curvature is large compared with the typical spacing between contact.

However, no definite criterion was given.

According to their proposition, it seems that the macroscopic contact geometry (i.e. curved contact interfaces) most likely has no influence at all. However, if the conventional analysis is applied beyond these conditions i.e. the radius of curvature is small, there may arise a great discrepancy between the calculated value and the real value. Therefore, consideration on the mascroscopic contact geometry should also be made in determining the thermal contact resistance.

The aim of this work is to study the thermal resistance between two concentric cylinders of different materials in contact with outward radial heat flow. To the author's best knowledge, no such work has been done before. An experiment is presented in studying the contact resistance with varying heat flux. Attempts to apply the conventional analyses to the experimental results are also made.

CHAPTER 2

REVIEW OF PARAMETERS AFFECTING THERMAL CONTACT RESISTANCE

The nature of heat transfer between two contacting metals may be said to have been well studied. However, due to a large number of factors affecting the thermal contact resistance, it is very difficult to obtain an accurate prediction on its value. Some of the main factors can be listed as follows:

(1) contact pressure,

(2) surface roughness and waviness,

(3) properties of contacting solids,

(4) mean interface temperature level,

(5) oxidation of contact surfaces,

(6) previous loading,

(7) direction of heat flux,

(8) interfacial fluid,

(9) mode of deformation.

Some of these factors have negative influence, i.e., tend to decrease the thermal contact resistance, while others have positive influence. In the study of one parameter, it is common to assume that the other parameters are constant, and therefore do not affect the discussion.

2.1 Effect of contact pressure

Among all parameters, the most significant one appears to be the apparent contact pressure. It is observed that the contact pressure has a negative influence on thermal contact resistance, i.e., as the contact pressure increases, the contact resistance decreases. The pressure dependence of contact resistance in the range of low pressure is more appreciable than in the range of high pressure. Fig. 1 shows schematically the influence of apparent contact pressure on the thermal contact resistance.

The basic concept of a contact process is that when two metal surfaces are brought close together, they begin to touch at the tips of the higher asperities. After the beginning of contact, the two surfaces approach closer to each other under an increase of the load. As a result of this, more protrusions come into contact and the size of the gap reduces. This implies that the real contact area and the number of contacts has increased. It has been observed that the rate of increase of real contact area is large initially, and then the rate decreases as the number of contact spots becomes large.

Correlation of the thermal contact resistance with apparent contact pressure in plane-contact surface models was studied in the literatures (16-23). It was found to be an inverse proportion, i.e. $R_c \propto P_a^{-m}$. The exponent varys from one to zero depending on deformation of the surface asperities.

2.2 Effect of surface roughness

Most engineering surfaces in engineering practice are wavy and rough. The relatively finely spaced irregularities of the surface are termed as roughness, and those with greater spacing are termed as waviness. Fig. 2 shows a typical linear profile of a wavy and rough surface. These surface irregularities are the result of the inherent action of engineering processes, machine or work deflection. Friction and wear which may take place at the interface will complicate the surface characteristics. The roughness formed under change of load has not been thoroughly understood, however it is believed to be taken care of by the contact deformation.

Consider two surfaces in contact, roughness is responsible for the microcontacts and because of the waviness these microcontacts are found in definite regions. By proper preparation of the surface, one can minimize the effect of waviness. However, one cannot completely remove the roughness even with superfinishing, therefore its influence does always persist.

It has been observed that the surface roughness has a strong effect on thermal contact resistance. Its influence is found to be positive, i.e., increasing the surface roughness increasing the contact resistance. In Fig. 3 the relation between contact resistance and surface roughness is illustrated. The dependence of contact resistance on roughness is strong when the load is relatively light and the surface are relatively smooth (small surface waviness), and less significant with high compression and wavier surface.

2.3 Effect of surface waviness

It has been proved that surface waviness has a positive influence on thermal contact resistance, that is, resistance increases with increasing surface waviness (surface flatness deviation). The influence is small for small waviness and becomes more pronounced for large waviness as illustrated in Fig. 4.

All engineering surfaces exhibit roughness and waviness. It has been observed that microscopic contact resistance is attributed to the surface roughness, and waviness is responsible for the macroscopic contact resistance. Some investigators showed that macroscopic contact resistance (waviness effect) dominates the overall thermal contact

resistance, whereas others observed that microscopic contact resistance (roughness effect) has commanding influence. It is very difficult to say whether roughness effect is larger than the waviness effect or not, because it strongly depends on the surface characteristics. Interaction between surface roughness and waviness was observed; roughness may act as negative influence on waviness. Generally speaking, since they are closely related, one cannot predict the thermal contact resistance without a knowledge of the interaction between them.

2.4 Effect of metal properties

As discussed earlier the thermal contact resistance is a combined effect of the surface conditions, thermal and mechanical properties of the mating materials, and the interfacial fluid. It is obvious that metal properties play an important part in determining the thermal contact resistance. There are essentially three kinds of related properties to be considered: thermal conductivity, hardness and modulus of elasticity.

2.4.1 Effect of thermal conductivity

It is found that the metal thermal conductivity has a negative influence on thermal contact resistance. Their relation has been well understood as practically linear. The reason why it is not exactly linear is because other properties such as hardness, Young's modulus and thermal expansion coefficient, will change as the thermal conductivity changes (Fig. 5).

2.4.2 Effect of hardness

By hardness we mean the pressure at which the material will yield under compression. It is a measure of resistance to identation. It has been observed to be responsible for the deformation mode, number and size of contacts. Its influence on the thermal contact resistance is positive and shown in Fig. 6. The variation is almost linear for very rough and flat surfaces.

2.4.3 Effect of modulus of elasticity

Attempts were made to correlate the thermal contact resistance with modulus of elasticity. It was found that the effect is significant when the surface irregularities undergo elastic deformation, and least or even zero when plastic deformation is governing. However, generally, the elastic modulus has a positive influence on the contact resistance, i.e., thermal contact resistance increases as elastic modulus increases, Fig. 7.

2.5 Effect of interfacial fluid thermal conductivity

Consider the contact of two bodies with presence of a conducting fluid in the interface, the thermal contact resistance may be determined by the relative proportions of the heat flowing through the real contacts and through the gap filled with fluid. This means the total thermal contact resistance is the sum of the direct contact conductance and the interfacial fluid conductance. It has been observed that there is a linear relation between the fluid thermal conductivity and the contact resistance. The fluid thermal conductivity has a negative influence on

the fluid resistance, and subsequently acts as a negative function of the overall thermal contact resistance, Fig. 8. The influence is extremely small at high vacuum.

At the interface the interfacial fluid can be a gas or a liquid. In general, the thermal conductivity of a liquid is higher than a gas. A significant reduction of resistance was found for the interfacial fluid being a liquid. The difference in contact resistance for the interface with a gas and for that with a liquid was attributed to an effective increase in the contact area [11] (see Fig. 9).

2.6 Effect of interfacial fluid pressure

Interfacial fluid pressure can be an important parameter in determining the thermal contact resistance of metals in contact with the presence of interfacial fluid.. The dependence of the thermal contact resistance on the fluid pressure is remarkable when the interfacial fluid is a gas. In the study of the gas pressure dependence of the contact resistance, Shlykov (34) carried out some tests with air over a large pressure range. The results showed that thermal contact resistance increases as the gas pressure decreases. A typical relationship between gas pressure and thermal contact resistance is shown in Fig. 10. It is seen from the figure that there are two horizontal levels and a transition. The lower level corresponds to the contact resistance at or close to atmosphere and the higher level is the contact resistance at high vacuum. The transition was observed over a very narrow pressure range and its change is nearly linear. It was also noted that the transition can shift and two horizontal resistance

level can change as well. This depends on many parameters, in particular apparent contact pressure and surface geometry. From the same diagram one can conclude that at high vacuum condition the fluid resistance is negligible and the entire amount of heat will flow through the place of actual metal contact.

2.7 Effect of mean interface temperature

The effect of the mean interface temperature on the thermal contact resistance is said to be well recognized. The influence of mean interface temperature is negative, that is contact resistance decreases when mean interface temperature increases, Fig. 11. At low temperature levels, say below $1000^{o}F$, the temperature effect for most metals is weak, but becomes significant as the temperature exceeds $1000^{o}F$.

Most of the material properties are temperature dependent at elevated temperature. Such a change in material properties will in turn cause a change in the deformation mode and the surface geometry, and consequently affect the thermal contact resistance.

In addition, at elevated temperatures the interfacial fluid thermal conductivity tends to change with the temperature level. Radiation heat transfer across the gap becomes significant, and the radiation resistance must be considered in determining the overall thermal contact resistance.

2.8 Effect of oxidation of contact surfaces

Oxidation is a common type of corrosion in metals. It results in formation of a thin oxide film covering the metal surface. The

growth of the oxide depends on the composition of metal, duration of exposure and environment conditions. The oxide, in general, has poor thermal conductivity and is less ductile than the pure metal. In addition, the oxidized surface is more irregular than that before oxidation.

The thermal contact resistance is found to be larger for oxidized surfaces than for pure metal contact. This is generally considered to be a function of the oxide properties (hardness, thermal conductivity), thickness of oxide film and the surface roughness after oxidation. Experiments and theoretical studies were carried out individually by Sanokawa (35) and Yip (32). The thickness and the thermal conductivity of the oxide film were found to be the main factors. Conclusions can be drawn as follows:

(1) Thermal contact resistance increases with increase in oxide film thickness, and the effect is enormous when the thickness approaches the value of pure metal surface roughness (Fig. 12).

(2) Thermal contact resistance tends to decrease as the thermal conductivity of oxide film increases.

(3) The effect is more pronounced when the surfaces are relatively smooth and contact pressures are light.

2.9 Effect of previous loading

The effect of previous loading, some called hysteresis effect, on the thermal contact resistance is recently of particular interest. It has been observed that at the same contact pressure, the thermal contact resistance in the initial loading application is higher than

that forming on descending loading. Figure 13 shows a typical variation of contact resistance with contact pressure for different loading conditions.

It is obvious that this effect is a result of the surface interaction. Mikic (13) presented a qualitative explanation for this phenomenon. He suggested that in the initial loading the deformation of the surface asperities is plastic, while in the descending loading the deformation is elastic. As the loading descends, part of the contacting asperities will recover and part will remain in contact, however, an overall effect of higher contact area under the same contact pressure will be obtained. Thus the difference of actual contact areas for the initial loading and the descending loading will certainly lead to the observed effect. It was also observed that the load dependence of contact resistance in the range of low pressure is more pronounced on initial loading than on subsequent (descending) loading.

2.10 Directional effect

By directional effect we mean the extent to which the thermal resistance of a contact between certain metals is influenced by the direction of heat flow across the interface. A first quantitative report of a directional effect between dissimilar metals in contact was presented by Barzelay et. al. (6). After that, several investigations have also revealed that there appears to be a significant directional effect between dissimilar metals.

Nevertheless divergent results by various investigators have been reported on the aluminum-stainless steel interface. Barzelay (6),

Roger (36) and Thomas (37) reported that: 1) the thermal contact resistance for the heat flow from aluminum to stainless steel is lower than when the heat flow in the other direction, and 2) there is an increase in directional effect with the contact pressure. Clausing (11) performed a more specific study on this topic and presented a different observation from those mentioned above. From his data he concluded that the thermal contact resistance was lower when the heat flows from stainless steel to aluminum. Williams (38) observed the same phenomenon. An elaborate work by Lewis and Perkins (12) was aimed at resolving all the previous conflicting results. They attributed the conflicts to different surface conditions (waviness and roughness) of their test specimen. They also pointed out that the both observed effects were correct as long as their respective contact surface conditions are considered.

There is some argument on the directional effects between similar materials. Williams (38) and Thomas (37) showed that a directional effect between similar materials was in fact observed, while Clausing (11) and Barber (39) suggested no directional effect. Moon and Keeler (40) presented a theoretical explanation of this directional effect by using the theory of heat transfer in the solid state. It reavealed that similar materials in contact can exhibit a directional effect if the contact surface histories are different.

To obtain an accurate estimate of this phenomenon, a better understanding of the surface interaction under different heating and loading conditions is necessary.

2.11 Effect of mode of deformation

By surface interaction we mean the mode of deformation of the surface asperities. It is generally assumed that the asperities of the contact surface undergo fully plastic deformation. This leads to the result that the actual contact area is directly proportional to the contact pressure. This assumption is not always true if the actual deformation process of the asperities is considered. Greenwood (22) pointed out that the contacts at the interface will in all states between fully plastic and fully elastic. He also showed that the deformation of the asperities is strongly dependent on the surface topography and the material properties.

Novikvo (25) correlated the thermal contact resistance and the contact deformation in the region of elastic and elastic-plastic contacts. He found that at low pressure the relation is an exponential function and becomes linear in the range of high pressure. This indicates that the contact deformation is elastic-plastic at low pressure and elastic at high pressure.

A more salient study on this effect was recently carried out by Mikic (26). He concluded that different modes of deformation have a significant effect on thermal contact resistance. Explicit expressions for the thermal contact resistance were derived for the cases of: 1) pure plastic deformation, 2) plastic deformation of the asperities and elastic deformation of the substrates, and 3) pure elastic deformation. In addition, a criteron was presented to determine the mode of deformation, Fig. 14, for given surfaces in contact. The effect of mode of deformation of the surface asperities is such that:

(1) under the same load, the thermal contact resistance is always higher for plastic deformation (Fig. 15),

(2) the contact deformation is not sensitive to the contact pressure level but depends on the surface conditions (roughness, average slope of the surface asperities) and material properties (hardness, elastic modulus).

2.12 Summary

From the above discussion the complexity of the thermal contact phenomenon is obvious shown. The parameters affecting the value of the thermal contact resistance can be divided into three important groups: 1) surface description (roughness, waviness), 2) surface interaction (mode of deformation) and 3) interstitial medium (interstitial fluid, oxide). Special care is required in determining the effect of one parameter. It is also obvious that some of the parameters cannot be determined without the knowledge of the others. Because of the large number of parameters affecting the thermal contact resistance, it is not surprising to see inconsistent and sometime conflicting results reported by different investigators.

CHAPTER 3

THEORETICAL BACKGROUND

3.1 Previous Theoretical Investigations

The evolution of the thermal contact resistance studies may be divided into three stages. They are:

(1) First stage: Emphasis was laid on the experimental values for each specific case (2-6, 36). All these works did not cover the particular materials and surface conditions of each other. Therefore, their applications were very limited.

(2) Second stage: Theoretical analyses were carried out on an idealized contact model as shown in Fig. 16 by Rapier et. al. (42), Ross and Stoute (43), Shlykov and Ganin (34), Sanokawa (9, 10), etc., who were aiming to obtain a better formulation for the thermal contact resistance. All these methods of calculation were based on the assumption that the contact surfaces are nominally flat, the actual areas of contact are uniformly distributed over the apparent area, the contact spots are all circular and of identical radius and the surface asperties deform plastically.

(3) Third stage: Further studies on the nature and interaction of the contacting surfaces indicated that reconsideration and modification of the theory were necessary. In order to modify the real surfaces in contact, considerations of surface parameters like surface roughness, surface waviness the distribution of surface slopes, and the deformation of surface asperities were included in the derivation. Some notable analysis on the non-ideal contacting surfaces were reported by Greenwood (22), Cooper et. al. (24), Clausing and Chao (45), Hsieh et. al. (44) and Mikic (26). To use

their formations detailed analysis on the profilometer traces of the surfaces in contact is generally required. These models, which have been well verified by experiments, can be applied to various contact joints, and give better explanations and estimate of the contact resistance.

The experimental data gathered by various investigations cannot be used to determine the thermal contact resistance if the joints (mating materials and surface conditions) are different from those investigated. However, they can be used for qualitative studies to show the trends as various parameters are changed. The theoretical analysis presented in Refs. (24, 26, 44, 45) are, of course, more likely to predict the exact value of thermal contact resistance of the real contacting surfaces. In such works many parameters are required to completely specify the mating surfaces. The surface roughness, the waviness (mean slope of surfaces) can be derived from profilometer traces. But in engineering practice, detailed information on the characteristics of the contacting surfaces may not be available, or may be too laborious to obtain from the profile analysis. Instead, some information, in the form of surface roughness readings, or merely the knowledge of manufacture process, is available. In this case, the approximate methods of calculation, though the accuracy may be a little inferior, may still produce useful results. Two such approximate models are discussed below and will be compared with the experimental results.

3.2 Theoretical Basis for Experiment

When heat flows across the interface of two members in contact, it is generally accompanied by an additional temperature drop which is

due to the imperfect contact at the interface. The thermal contact resistance is defined by Eq. (1) as:

$$R_c = \frac{\Delta T_c}{(Q/A_\alpha)}$$

The heat flow rate, Q, is determined by the temperature distribution in the undisturbed region. The additional temperature drop, ΔT_c, is obtained by extrapolating the temperature distributions in both contacting members from the undisturbed region to the interface. A_α is the apparent contact area.

3.3 Formulation of Analytical Models

The heat transfer across the contacting surfaces may be considered to consist of two components:

(1) heat conduction through the direct contact spots,

(2) heat conduction through the interfacial medium.

The total thermal contact resistance, R_c can therefore be defined by the thermal resistance of direct metal contact, R_M, and the thermal resistance of the interfacial medium, R_F. Assuming one has negligible effect on the other, the total thermal contact resistance can then be represented by the equation for parallel resistors:

$$\frac{1}{R_c} = \frac{1}{R_M} + \frac{1}{R_F} \qquad (2)$$

Now the problem of determining the total thermal contact resistance reduces to a separate estimation of its components.

Here two models, Shlykov and Ganin model, and Ross and Stoute model, are used to determine the thermal resistance of metal contact

and a simple expression derived by Shlykov and Ganin is used to describe the thermal resistance of the interfacial medium. The final equations for the thermal contact resistance can be obtained by combining the expressions for each component.

3.3.1 Shykov and Ganin Model

Presumption: (1) The contact surfaces are nominally flat.

(2) Plastic deformation at the surface asperities.

(3) The size of the contact spots is independent of loading.

The contact spots are circular with radii about 30 μ.

The equation for the thermal contact resistance (R_c) is given as:

$$\frac{1}{R_c} = \frac{2\,k_f}{\sigma_1 + \sigma_2} + 5.3906 \times \frac{k_M P_c}{c\ \sigma_B} \times 10^{-2} \left(\frac{\text{sec in}^2\ ^\circ F}{\text{Btu}}\right) \qquad (3)$$

where k_f = thermal conductivity of interfacial fluid

k_M = harmonic mean thermal conductivity $\left(\frac{2\,k_1\,k_2}{k_1 + k_2}\right)$

P_c = contact pressure

C = coefficient

σ_B = ultimate strength

σ = surface roughness of contacting interface

3.3.2 Modified Ross and Stoute Model

The expression of the thermal resistance of direct metal contact is quoted from Ross and Stoute (43). Regarding the expression of the thermal resistance of interfacial medium, instead of using the original one given in (43) the one developed by Shlykov and Ganin (34)

was used because the latter was found to be much convenient to use. The basic assumption is the same as Shlykov's, except that the radius of the contact spot, a, is given in terms of surface roughness, σ, and is given as:

$$a = a_o \sigma^{1/2} \tag{4}$$

where:

$$a_o = 0.31375 \text{ in}^{1/2} \text{ (or } 0.5 \text{ cm}^{1/2}\text{)}$$

The thermal contact resistance (R_c) for this situation is:

$$\frac{1}{R_c} = \frac{2\ k_f}{\sigma_1 + \sigma_2} + \frac{k_M}{a_o\ \sigma^{1/2}} \left(\frac{P_c}{H}\right) \left(\frac{\text{sec in}^2\ {}^oF}{\text{Btu}}\right) \tag{5}$$

where k_f = thermal conductivity of interfacial fluid

k_M = harmonic mean thermal conductivity $\left(\frac{2k_1\ k_2}{k_1 + k_2}\right)$

P_c = contact pressure

σ = surface roughness

H = microhardness

CHAPTER 4

EXPERIMENTAL APPARATUS AND PROCEDURE

4.1 Description of Apparatus

The experimental apparatus is shown in Fig. 17. A close-up view of the test set-up is also shown in Fig. 18.

The apparatus consisted of a test specimen, which is an aluminum-stainless steel compound cylinder, to provide the interface for the study. The specimen was made by shrinking the aluminum cylinder onto the stainless steel cylinder. Its dimensions are 5.68 in. in length, 0.875 in. inside diameter and 2.875 in. outside diameter. At each end of the specimen there were a teflon and a steel guard plate. The teflon guard plate served as thermal insulation to minimize the longitudinal heat loss, and the steel guard plate was designed to guide the thermocouple wires out from the specimen. Aluminum centering bushings were placed through the guard plates into the recesses at the ends of the specimen. This assembly was then placed on the lower base plate such that the centering bushing stood in the recess of the base plate; and on the top of it sat the upper base plate. The specimen was constrained at both ends simply by tightening the base plates on to the steel sheel.

A 13 in. long stainless steel heating element of 3/4 in. diameter and 0.035 in. thick was placed through the centre hole of the specimen in such a way that a 1/16 in. gap is left between the heating element and the specimen. Each end of the heating element was clamped tightly by a piece of brass terminal block. The top terminal block was bolted to the upper steel base plate, and it was hanging freely at the bottom. The purpose of the asbestos ring, numbered 15 in Fig. 17,

was to prevent the heating element from moving sideways. On the top of this and in between the heater and the steel ring was a thermal insulation sleeve, numbered 14, serving to eliminate the heat loss through the hanging end of the heater. The inside of the heater was filled with thermal insulation. The voltage was supplied to the heater by means of a Raytheon Company, Sorensen Operation, Three Phase Input Power Supply Model DCR 20-1000 A (See Fig. 19). Heat flowed radially outward through the air gap and the specimen.

Tap water was circulated on the outside of the specimen, and a close-up jacket (Fig. 20) was designed to stabilize the water flow. Thermocouples, details of which are given in section 4.3, were taken out of the apparatus through the conax seals (MHC-040-8) supplied by Conax Corporation. Fig. 21 shows the sectioning view of the conax seal. When the assembly was tightened, the compressed teflon seals which were placed at the ends of the center bushings formed an effective seal against the centering bushing and the recess. These seals when desired to replace the specimen had to be dismantled.

A thermal insulation jacket about 1 1/2 in. thick was also provided to wrap around the hanging heater terminal.

4.2 Preparation of Test Specimens

The test specimen was made from two concentric cylinders by a process called "cold fits". The materials of the test pieces were aluminum 2011-T351 and stainless steel type 304. The mechanical and physical properties for these are given in Table 1 and 2. They were selected on the basis of the following conditions:

(1) a larger coefficient of thermal expansion for the inside cylinder than that for the outside cylinder,

(2) popularity in aircraft and industry applications,

(3) availability of the materials.

The outside surface of the aluminum cylinder was turned on a lathe to a specified roughness range, and the inside surface of the stainless steel was as received. A tracer-type Brüel and Kjaer Roughness Meter Type 6102 and coupled with a Motor Drive Type 3910 for roughness meter was used to measure the roughness of the test pieces. Pertinent information regarding the dimensions and the surface roughness of individual test pieces is given in Table 3.

The stainless steel cylinder has an internal diameter slightly less than the external diameter of the aluminum cylinder. To assemble them a shrink fit process had to be used. It is known that aluminum will change its properties at elevated temperature but remain the same at sub-zero temperature. It was also required that no damage to the contacting interface should result from the assembling process. Therefore, a cold fit was employed to assemble the test pieces. The aluminum, with its machined to the exact dimension and desired roughness, was immersed into a container of liquid nitrogen to cool to about $-200^{o}F$. It was then taken out to fit the stainless steel cylinder. Special care was given during assembling. After the assembly warmed up it was then machined to the required dimensions.

An initial contact pressure which depends on the interference was introduced at the interface during the process, and this can be determined by the theory of elasticity.

4.3 Thermocouple Technique and Preparation of Thermocouple Wells

Since the accuracy of the evaluation of the thermal contact resistance depends on accurate temperature measurement, much attention was given to the positioning of thermocouples and preparation of thermocouple wells in the experiment. It is known that thermocouples have to be placed at a transverse section in the heat path, therefore the thermocouple wells were drilled longitudinally down to the desired depth from the end surfaces. Two methods of preparing the thermocouple wells were attempted and details are discussed in section 4.3.2 and 4.3.3.

The basic requirements for thermocouple wells were:

(1) The size of hole should be fine enough to fit the thermocouple and without producing any disturbance in the heat path.

(2) The holes must be straight and vertical to the heat path.

(3) The variance in depth of the holes must be less than a tolerance of $\pm$ 1/2 (hole size).

4.3.1 Thermocouple Mounting Technique

The thermocouple mounting technique was similar to that of Clausing and Chao [45], but with several modifications.

ISA JJ No. 30 gauge iron-constantan thermocouple wire was used for the temperature measurement. The bead was formed by a mercury thermocouple welder, and it was sprayed with a very thin "Rid Arc" coating to provide protection and electrical insulation. A small piece of lead foil about 0.003 in. thick was wraped around the thermocouple to ensure that the thermocouple was centrally located in the hole. It

was then inserted into the hole until touching the bottom. The top of the hole was filled with epoxy which when hardened served to hold the thermocouple in place. A sketch of the thermocouple installation is shown in Fig. 22.

By use of a spot welder thermocouples were welded on the skin of the specimen to measure the surface temperature.

4.3.2 Preparation of Thermocouple Wells in Specimen TCR-1

In the specimen TCR-1, fifteen thermocouple wells 1/16 in. diameter were drilled by a drilling machine on three different levels. The top and mid levels were 1 1/2 in. and 2.8 in. from the top end respectively, and the bottom level was 1 1/2 in. from the bottom end. On each level three holes were drilled in the aluminum and two in the stainless steel (Fig. 23). A 1/16 in. diameter long series drill was used, and special care was given during drilling. Great difficulties were encountered in the drilling process because the drilling machine was not capable of drilling such fine and deep holes, especially when drilling the stainless steel piece. It was soon found that three thermocouple wells at the top level and two at the mid level were unsatisfactory because of scatter of the measured temperature. Accordingly only the data recorded on the bottom level was used for the calculation.

4.3.3 Preparation of Thermocouple Wells in Specimen TCR-2

To obtain better results, the method of drilling the thermocouple wells had to be improved or an alternative method found. It was also desirable to reduce the hole size to be just sufficient to take

30 gauge thermocouple wires. A spark cutting machine, (Agemaspark Eurospark Machine Type F400P-20) shown in Fig. 24, was employed for preparing the thermocouple wells for the specimen TCR-2.

The principle of operation of the Eurospark Machine is that it removes metal from the area in the immediate vicinity of the tool without mechanical contact with the work by generating a rapid series of spark discharges of controlled energy between the tool and the work. The sparks erode a small crater of metal by melting and vaporization. The advantages in the present application are: 1) its ability to machine hard material such as stainless steel, 2) its ability to bore very fine hole, 3) its ability to machine to any finished shape and to cut starting at any angle to the work surface. The only disadvantage (as experienced in this study) was that it consumed too much time. This occured because the cutting speed slowed down as the tool cut deeper.

A special tool holder was designed for the purpose of multi-element drilling and is shown in Fig. 25. Ground finish tungsten electrodes of 0.040 in. diameter and 5 in. long were soldered on to the tool holder. Before drilling specimen TCR-2, a practice run was made on a dummy specimen. A few holes were first drilled on both aluminum and stainless steel test pieces to a depth of about 1 1/2 in. These showed that the holes were very straight and the size of the holes was about 0.010 in. larger than the tool size (See Fig. 20). A photograph of the specimen TCR-2 during drilling is shown in Fig. 26.

At each level, five and three holes were drilled in the aluminum and stainless steel respectively. The thermocouples protruded from the

holes were embeded in the grooves on the end surface in such a manner that they could be grouped into a bundle (See Fig. 27). This bundle was then taken out through the conax seals to the measuring devices. Seven thermocouples were spot-welded on the outside surface to measure the skin temperature as shown in Fig. 28. Fig. 29 shows the location of the thermocouple wells for specimen TCR-2.

4.4 Equipment for Experiment

4.4.1 Power Supply

To supply the voltage to the heating element a three phase input power supply model DCR 20-1000 A (Fig. 19) supplied by Raytheox Co., Sorenson Operation, was used. This power supply provides a stable, highly regulated dc output from a wide range of three phase input voltages and frequency. The output ratings are 0-20V and 0-1000 A. Coarse and fine voltage adjustment controls were provided to assure the selected output voltage. The unit also incorporates three protection systems: phase-failure shutdown drops the output automatically to zero when failure of any input phase occurs; thermal overload shutdown also drops the output to zero if the unit is overheating; automatic crossover system provides current limiting protection. In addition, other features such as remote programming, remote sensing series and parallel operation are also built in the unit.

4.4.2 Flow Meter

In order to maintain a constant flow of cooling water passed over the specimen, a flow meter supplied by Schattle and Koerting Co. (Fig. 30) was used. The maximum rating is 17 gpm, and for this experiment

the optimum flow rate was found to be 6 gpm.

4.4.3 Temperature Measuring Devices

No. 30 gauge iron-constantan thermocouples were installed in each specimen for the temperature measurement. The thermocouple monitoring system consisted of a DANA Laboratories, Inc. digital multimeter model 5000 and a Leeds & Northrup Co. model S 60000 series Speedomax G recorder. The former recorded the temperature readings, while the latter was used to record the continuous change of the temperatures and also as a steady-state indicator. A key switch module was also provided for converting the single point measuring instrument to a multipoint unit.

In conjunction with the above mentioned instruments a reference junction supplied by Thermo-Electric Co., Inc. was also used.

4.4.4 Voltmeter

Although the voltage supplied to the heating element can be obtained from the null voltmeter in the power supply unit, it was more convenient to read out from a large, easy-view face null voltmeter. Therefore, a Hewlett-Packard model 419A dc null voltmeter was employed. This model also has the selectable voltage span to match the voltage sources.

4.5 Test Procedure

Fig. 32 is a photograph of the test equipment installation. Before starting a test, the reference junction unit, the Speedomax G recorder, and the digital multimeter usually had to warm up for about an hour. The power supply was then switched on to the desired power

level and a constant flow of cooling water was circulated over the specimen. The system usually took 2-3 hours to attain steady state conditions. The Speedomax G recorder was primarily used to indicate when thermal equilibrium was reached. A complete set of thermocouple readings was taken using the digital multimeter and a key switch unit at intervals of 10 minutes, until four successive sets of data agreed to within 1 percent. The procedure was repeated for other power levels. The maximum value of heat flow across the specimen was governed by the maximum operating temperature of the stainless steel heating element. The power rating ranged from 0.25 to 2 KW; in practice heat flux across the interface ranged between 1840 and 14000 Btu/hr ft^2.

In this study the interface contact pressure consisted of two components; an initial contact pressure built up at the interface during the cold fit process and a thermal contact pressure introduced by the differential thermal expansion of the respective test pieces during the tests.

CHAPTER 5

ANALYSES AND EXPERIMENTAL RESULTS

5.1 Calculation of Thermal Contact Resistance

Heat flow across the test members was calculated from the known thermal conductivities and the associated temperature gradients. For the test covered, the difference between them usually did not exceed 10 percent. For a few data points the difference was as high as 15 percent. The mean value of heat flow across the test members was used for the calculation of thermal contact resistance.

The temperature gradient in the aluminum test piece was obtained by the method of least squares approximation, and extrapolation yielded the aluminum interface temperature. Using the heat flow for the aluminum cylinder, the stainless steel interface temperature was determined by:

$$T_c = T_2(r) + \frac{Q \cdot \ell n(r/r_2)}{k_2} \qquad (6)$$

The interface temperature drop was calculated as the difference in the interface temperatures of the two test members. Thermal contact resistance was evaluated by using Eq. (1).

5.2 Determination of Contact Pressure

Initial Contact Pressure

In the cold fit process an initial contact pressure was built up at the interface when the aluminum cylinder was shrunk onto the stainless steel cylinder. This contact pressure depends on the amount of interference of the mating cylinder, the radii, and the material properties of the components. This problem has been well studied in the literature (46).

For a given interference and the known mechanical properties of the mating pieces, the initial contact pressure P_{sc} was calculated by (Appendix B)

$$P_{sc} = \frac{\delta/2}{r_2 \left[\frac{1}{E_1}\left(\frac{r_2^2 + r_1^2}{r_2^2 - r_1^2} - \nu_1\right) + \frac{1}{E_2}\left(\frac{r_3^2 + r_2^2}{r_3^2 - r_2^2} + \nu_2\right)\right]} \qquad (7)$$

where δ = interference

r_1 = inside radius

r_2 = interface radius

r_3 = outside radius

E = Youngs modulus

ν = Poisson's ratio

Thermal Contact Pressure

Thermal stresses were set up in the specimen during the test due to its non-uniform temperature gradients. Thermal contact pressure is defined as the thermal loading at the interface exerted by one cylinder on the other. The derivation of the thermal stresses in the composite cylinder and the formulation of the thermal contact pressure are described in Appendix B. The theoretical analysis of thermal stresses in a composite cylinder is based on the following assumptions:

(1) The temperature distribution is taken to be axisymmetric and independent of the axial coordinate.

(2) Since the ends of the specimen were well confined between fixed rigid base-plates, plain strain condition is considered to be well justified.

With the measured temperature distribution and the calculated thermal contact resistance, thermal contact pressure P_{tc} can be determined by:

$$P_{tc} = \frac{e_2\, e_3\, A(r_2^2 - r_1^2) - e_1 \alpha_1 h_1}{r_2^2} \tag{8}$$

or

$$P_{tc} = \frac{e_4\, \alpha_2\, h_2 - e_5\, e_6\, D\, (r_3^2 - r_3^2)}{r_2^2}$$

where coefficients e_1, e_2, e_3, e_4, e_5, e_6, h_1, h_2, A and D are given in Appendix B.

Total Contact Pressure

Since no plasticity exhibited at the interfaces of the test specimen or elsewhere in all the tests conducted in this investigation the principle of superposition can be used for determining the total contact pressure. The total contact pressure P_c is therefore the sum of the initial contact pressure and the thermal contact pressure.

$$P_c = P_{sc} - P_{tc} \tag{9}$$

5.3 Presentation of Results

It is important to point out that results for the top and mid levels on both specimens were being neglected. Experimental analysis showed that the scatter in the temperature data for these two levels was large, and the results were too poor for the calculation of thermal contact resistance. Details are discussed in the next chapter. Thus, only the results of the lower level for each test are presented here.

The experimental results of the thermal contact resistance of an aluminum-stainless steel composite cylinder are given in Table 4. This table records the heat flow through the composite cylinder, the temperature drop across the interface, the calculated thermal contact resistance and contact pressure for each test. In addition, the values of thermal contact resistance calculated by the proposed models, Eq. (3) and Eq. (5), are also presented.

The series of tests designated as TCR-2.XR were repeated on specimen TCR-2 to check reproducibility of the results.

Experimental data are also presented in the form of diagrams. Fig. 33 to 35 are the temperature distribution for each specimen. The mean contact temperature ranged between 61-112^{o}F. Fig. 36 shows thermal contact resistance vs. heat flux across the interface, while Fig. 37 shows thermal contact resistance vs. contact pressure.

Comparisons of the experimental results and the proposed analytical models are presented in Figs. 38 and 39. In calculating the thermal resistance of the interfacial medium, air was taken as the interface gas. Figs. 40 and 41 show the variation of thermal contact resistance with contact pressure.

CHAPTER 6

DISCUSSION OF RESULTS

6.1 Scatter of Data

In analyzing the experimental data, it was found that the scatter of the thermocouple readings from the top and mid levels for both specimens precluded their use in calculating the thermal contact resistance. This scatter arose from two factors: 1) the uncertainty in thermocouple position, and 2) the uncertainty of contact between the thermocouple bead and the lead foil.

Uncertainty in thermocouple positions can be due to uncertainties in the position of the thermocouple in its hole and of the position of the hole itself. Inspection of specimen TCR-1 showed that these problems largely accounted for the observed scatter of the data points on these two levels. For specimen TCR-2, the position of the thermocouple wells was quite satisfactory. Scatter in the temperature, however, was recordered again, the worst being the mid and top levels. Certain tests appeared reasonable but on the whole readings at these levels were not satisfactory. In searching for the reason, it was found that the lead foil which wraped around the thermocouple could be easily moved along the thermocouple. As the lead foil was tamped down a little more, it certainly caused contact with the thermocouple bead. Further, the thermocouple with the foil was not a good fit to its hole and contact between the lead foil and the hole occured at discrete points. This accounted for the observed scatter.

6.2 Error Analysis

This section contains a discussion of the systematic and random errors which occured in the experiment and their effects on the correlation of results.

6.2.1 Error Analysis of Apparatus

The error analysis of the effect of temperature uncertainties on thermal contact resistance was made on a single-sample experiments basis proposed by Kline and McClintock [64]. The method and the sample calculation are given in Appendix A.

The errors in the temperature measurements were estimated from the calibration error of thermocouples, instrument error, and the uncertainty in positioning the thermocouple in the hole. The errors as obtained from the manufacturer's data on the thermocouples and the digital multimeter were:

$\pm$ 1/2% of the temperature read out of the thermocouples

$\pm$ 0.01% of the DVM readings

At the lowest thermal contact resistance, that is test 1.6, the temperature gradients of about $0.02^{o}F$ per thousandth of inch and about $0.11^{o}F$ per thousandth of inch existed in the aluminum and stainless steel cylinders respectively. The uncertainty in the thermocouple positions in the wells was estimated to be 0.010 in. i.e. + 0.005 in. This accounted for an error of about $\pm$ 1 percent of temperature readings.

It was discussed previously that the difference between the heat flows for the aluminum and stainless steel pieces was usually not in the excess of 10 percent, and the average value of heat flows was used in the calculations of thermal contact resistance. Therefore, the fractional uncertainty in the radial heat flow, as the worst case was considered, was taken as $\pm$ 5 percent of the mean value.

By taking into consideration of all these uncertainties in the temperature measurements, the percentage error in the experimental values

of thermal contact resistance was ± 5.22 percent. Correction was applied to the experimental data in the form of error band, and it is shown in Figs. 36 and 37.

6.2.2 Error Analysis of Theoretical Models

The following is an error analysis of the effects of the uncertainty in temperature measurements and the uncertainty in contact pressure on the theoretical predictions. The effect of the temperature uncertainties on the theoretical predictions is the same as discussed in the previous subsection. The effect of contact pressure uncertainties mainly arose from the uncertainty in the cold fit due to the uncertainties in cylinder dimension measurements.

In the dimension measurements for the test cylinders, the errors in measuring the interface radii is the most important factor that would cause uncertainty in contact pressure. Such errors in turn caused some additional scatter in determining the theoretical results. The percentage error in the interference on the basis of twenty measurements on each test piece was taken as ± 5 percent. The uncertainty in contact pressure due to the uncertainties introduced in interference corresponded to a percentage error in the theoretical results of ± 1.54 percent for test TCR-1 and ± 1.00 percent for test TCR-2.

Taking into account of the effects of temperature uncertainties and contact pressure uncertainties an error band was applied to the theoretical results for each analytical model. This is shown in Figs. 38 to 41. The average percentage error based on the six tests of each of the two specimens was: 5.68 percent for specimen TCR-1, and 6.02 percent for specimen TCR-2.

6.2.3 Errors in Roughness Measurements

A tracer-type Brüel and Kjaer roughness meter type 6102 coupled with a motor drive type 3910 for roughness meter was used to assess the roughness of each test surface. Information regarding the surface roughness of each test piece is shown in Table 3. The percentage difference of surface roughness σ ($= \sqrt{\sigma_1^2 + \sigma_2^2}$) was about 22 percent for specimen TCR-1 and about 12 percent for specimen TCR-2. The error in the surface roughness measurement was found only to be responsible for the calculation of the interfacial fluid resistance and metal resistance term in the modified Ross and Stoute model. This is easily shown by checking Eqs. (3) and (5). As a rough approximation, the percentage difference in the interfacial fluid resistance was 20.0 percent for TCR-1 and 12.1 percent for TCR-2. The corresponding percentage error in the theoretical values of R_c would be 9.96 percent and 7.85 percent for TCR-1 and TCR-2 respectively. For the percentage error in the metal resistance in the modified Ross and Stoute model was found to be negligible. Accordingly, the percentage error in the theoretical results due to the temperature uncertainties, contact pressure uncertainties and errors in roughness measurement was estimated to be 9.89 percent for TCR-1 and 11.47 percent for TCR-2.

6.2.4 Systematic and Random Errors

Systematic Errors

In the present experiment systematic errors in the calculated thermal contact resistance would arise from an assumption of constant metal thermal conductivity and from the longitudinal heat loss.

Throughout this study, the thermal conductivities of aluminum and stainless steel were assumed to be temperature independent. This was not actually true since they vary with temperature. However, the error introduced by assuming the thermal conductivity to be constant was insignificant because its variation with temperature over the temperature range under testing was very small.

Temperature gradient along the length of the specimen was measured for both specimens. This was probably because 1) an isothermal boundary condition at the outside surface of the test specimen was not completely satisfied, and 2) natural convection took place in the enclosure between the heater and the specimen. The worst error occured in the test 1.6 where the longitudinal temperature gradient was about 2.4 percent of the radial temperature gradient. This, however, caused a negligible error in the results of thermal contact resistance.

Random Errors

Other error contributions to the total inaccuracies of the results are classified as random errors. One possibility was the variation in the degree of contact between thermocouple beads and the bottom of the well which would cause appreciable error while testing at a lower temperature range. Another error can be attributed to the thermocouple contamination and the perturbation of heat flow by the thermocouple and the will. Another possibility is the eccentricity of the heating element, which, could cause non-uniform heat transfer in the circumferential direction. Since no measurements were made to study these effects, their magnitude remains indeterminate.

6.3 Discussion

Fig. 36 gives the results of the experiment; thermal contact resistance being plotted against the heat flux across the interface with

surface roughness as a parameter. It can be seen from the figure that thermal contact resistance of a compound cylinder decreases with increasing heat flow through the cylinder. As the heat flow increases, thermal strain is set up at the interface, and this in turn causes an increase in contact pressure. The result, therefore, is actually the combined effect of the heat flow and contact pressure. Since there is no published data available for comparing and verifing the experimental results, one may ask: do the results show the right trend? According to experimental studies by Thomas and Probert (37) and Rapier et. al (42), thermal resistance for direct contact was not noticeably dependent on heat flow. The effect of heat flow on the thermal resistance of the interface medium, in the contact temperature range covered here, was weak. Applying this conclusion to the present results, a trend of decreasing thermal contact resistance with increasing contact pressure can be drawn (Fig. 37). Thus, the experimental results exhibit trends consistent with the literature. The effect of the surface roughness is also presented in the diagram. The influence is positive, i.e. thermal contact resistance increases as the surface roughness increases.

The results for tests TCR-2.XR agree very well with that for tests TCR-2.X. The reproducibility and consistency are clearly shown by this diagram. No hysteresis effect was observed in the test range covered.

Comparisons of the present work with the analytical models discussed in section 3.3 are made in Figs. 38 and 39. In these figures experimental values are shown in solid lines and analytical values in broken lines. One can see that there are significant differences between the experimental data and results of the analytical calculations. The slope of the experimental

curves happens to be a little sharper than that of the analytical curves. These phenomena are not unreasonable if it is borne in mind that the conventional analysis made no attempt to consider the geometry effect of this particular contact configuration.

In order to attain an explanation for the phenomena, let us consider the thermal resistance of direct metal contact. In the conventional test apparatus the mechanical loading system was set up in such a manner that it enabled free expansion of the test pieces in the lateral direction. Thermal resistance of direct metal contact was found to be invariant with heat flux. At moderate heat flow this might be possible because the thermal strain at the interface could be too small to change the contact surface characteristics. If the heat flux is extremely large, the effect will be significant. Since the thermal strain is compressive it is no doubt that an additional thermal resistance will result. In the case of a cylindrical interface of a compound cylinder, the amount of compressive thermal strain at the interface will be much larger than that exhibited in the plane-contact interface of the conventional models under the same conditions of heat flux and contact pressure due to the constrained interface boundary. Its effect, then, may not be insignificant. It will be more pronounced in the case where an extremely large heat flux passes through the interface.

Consider a cylindrical interface of two contacting members as shown in Fig. 42; heat flows radially outward in the 1 - 2 direction. The interface of region 1 will be at a higher temperature, and thus expands. The contacting portion will squeeze the interface of region 2 causing a large contact pressure and the void will be closed in upon the opposite interface. As a result of this there will be an increase in contacting

area and a decrease in gap size, and thus a decrease of thermal resistance results. Consider another physical model as shown in Fig. 43, with the discontinuity in the low conductivity material - stainless steel. If the radial outward heat flow if from 1 to 2, the portion of region 1 opposite the discontinuity will be at a higher temperature and expand into the discontinuity. This will reduce the gap size, and causes a decrease in thermal resistance. Such geometric effects could be significant because of the large thermal strain built up at the cylindrical interface. Referring to this experiment, the specimen TCR-1 fits the former physical model and specimen TCR-2 fits the latter. As for the thermal resistance of the interfacial medium, the effect of thermal strain due to the heat flux was small, in particular, for the test range covered here. It can be seen that the discrepancy between the experimental values and the analytical results may be attributed to the different amount of geometric effect of thermal strain.

Fair agreement between the two proposed models can be seen in Fig. 39, but in Fig. 38 the agreement is poor. In the Shlykou and Ganin model a constant spot radius of 30 μ (1.18×10^{-3} in.) was assumed; whilst in the modified Ross and Stoute model the contact spot radius was replaced with a function of surface roughness. If the surface roughness exceeds 14.175 μ in., the value of thermal contact resistance calculated by the Ross and Stoute model will always be larger than that determined by the Shlykov and Ganin model. They will diverge as the surface roughness increases.

The contact pressure can be calculated by Eq. 9. Diagrams of the thermal contact resistance against contact pressure were plotted and are given in Fig. 40 and 41.

CHAPTER 7

CONCLUSION AND RECOMMENDATION

7.1 Conclusion

The present investigation has demonstrated the effects of contact pressure and surface roughness on the thermal contact resistance of a compound cylinder. No published literature could be found on this specific type of structure. The effect of contact pressure is negative, i.e. contact resistance decreases with increasing contact pressure, and the effect of surface roughness is positive, ie. contact resistance increases with surface roughness.

Experiment evidence indicates that the heat flux, which is usually considered to have little or no effect on the thermal contact resistance for plane-contact surface models, plays an important role in determining the thermal contact resistance of a composite cylinder. It is suggested that discrepancies between the experimental values and the results of two conventional plane-contact surface analytical models are attributed to the geometric effect on the deformation at the interface caused by heat flux induced thermal strain. Two physical models are postulated to explain this effect.

The trends shown in Figs. 36 and 37 are reconcilable with the concept that the contact pressure causes microscopic deformations of the surface asperities which is further aggravated by the compressive thermal strain. It is also suggested that the plane-contact surface analytical models can be applied to contacts between concentric cylinders with a sufficient degree of accuracy provided that the effect of the thermal strain is taken into consideration.

7.2 Recommendations

It must be emphasized that the present work is a preliminary study on the thermal contact resistance of a compound cylinder. Effects

of many parameters such as the surface waviness, interfacial gas, oxidation of contacting surfaces and so on have not been examined in this experiment. Further work is necessary to assess these aspects and obtain a better understanding of the thermal contact resistance of a cylindrical-contact interface. Of particular interest is the quantative evaluation which is of considerable importance in the sense of engineering design; qualitatively the trends of these effects can be well described by the conventional plane-contact surface analysis.

In view of this work a number of recommendations can be made on the test apparatus, test specimen and possible further work on this particular contact configuration. Considering the test apparatus, it is recommended that the heating element be modified to provide larger heat flow to the specimen such that tests can be extended to much higher interface temperature levels. The disadvantages of the present heating element are: 1) it could not supply a large heat flow at the temperature required because of the large radiative area ratio, and 2) heat leaked from the free end of the terminal even though an insulation jacket was wraped around the terminal. To overcome these, either modification to the heater terminals and the heater itself or a new design of heater should be made. A thin-walled type heating element which is made of stainless steel shim of about 0.005 in. in thickness would be considerably as a radiant heater for further work. In addition, helium gas with its higher thermal conductivity could also be introduced into the enclosure between the heater and the specimen to improve the heat transfer conditions.

As regarding to the test specimen, it is suggested that it should be changed to a disc-like composite cylinder such that the thermocouple

wells would be much easier to prepare and the thermocouple positions would be more accurately controlled and known. This is particularly important since the accuracy of the determination of thermal contact resistance depends heavily on how accurately thermocouple positions are known. However, if the same type of specimen is used, the spark erosion machine is highly recommended for drilling the holes, but a special design for the multi-element tool holder must be made.

As the last recommendation on this work, further study should be made on this particular contact geometry. It was realized that only two specimens with different surface roughness were tested. Such a limited number of observations was, of course, insufficient to make a comprehensive study on the geometry effect of the cylindrical interface on the thermal contact resistance. It is suggested that more specimens should be tested. Tests could also be done on specimens with smaller ratio of radius of curvature to interfacial gap. The major uncertainty in determining the thermal contact resistance by use of the analytical models is the value of contact pressure. Present study calculated the contact pressure based on the theory of elasticity, but no measurement was done to assure its value. Some further work in this area is required. For example, residual stress measurement could be performed on the cylinder system to determine the actual value of initial contact pressure introduced in the cold fit process, and strain-gauges could be mounted on the outside surface of the specimen such that the interface contact pressure could be assessed. One other task that should be undertaken would be to conduct tests at constant heat flow but with varying contact pressure by applying high gas pressure to the inside cylinder. In this case, the present test apparatus should be modified to accomodate

varying gas pressure. However, such effort may well be worthwhile for the better understanding the relationship between contact pressure and thermal contact resistance.

REFERENCES

1. A.M. Clausing and B.T. Chao, "Thermal contact resistance in a vacuum environment", Univ. of Illinois, Eng. Exp. Stat. Report ME-TN-242-1, 1963.

2. R.B. Jacobs and C. Starr, "Thermal resistance of metallic contacts", Rev. Sci. Instru. vol. 10, 140-141, 1939.

3. N.D. Weills and E.A. Ryder, "Thermal resistance measurement of joints formed between stationary metal surface", Trans. ASME vol. 71, 259-267, 1949.

4. A.W. Brunot and F.F. Buckland, "Thermal contact resistance of laminated and machine joints", Trans. ASME vol. 71, 253-357, 1940.

5. M.E. Barzelay, K.N. Tong and G.F. Hollo, "Thermal conductance of contacts in aircraft joints", NACA TN-3167, 1954.

6. M.E. Barzelay, K.N. Tong and G.F. Hollo, "Effect of pressure on thermal conductance of contact joints", NACA TN-3295, 1955.

7. H. Fenech and W.M. Rohsenow, "Thermal conductance of metallic surfaces in contact", U. S. A.E.C. Report NYO-3126, 1959.

8. L.C. Laming, "Thermal conductance of machined metal contacts", Int. Develop. in Heat Transfer, ASME International Heat-Transfer Symposium, Boulder, Colo., 65-76, 1961.

9. K. Sanokawa, "Heat transfer between metallic surfaces in contact", 1st report, Bulletin of J.S.M.E. vol. 11, no. 44, 253-263, 1968.

10. K. Sanokawa, "Heat transfer between metallic surfaces in contact", 2nd report, Bulletin of J.S.M.E. vol. 11, no. 44, 264-275, 1968.

11. A.M. Clausing, "Heat transfer at the interface of dissimilar metals: - the influence of thermal strain", Int. J. Heat Mass Transfer 9, 791-801, 1966.

12. D.V. Lewis and H.C. Perkins, "Heat transfer at the interface of stainless steel and aluminium: - the influence of surface conditions on the directional effect", Int. J. Heat Mass Transfer 11, 1371-1383, 1968.

13. B.B. Mikic, "Analytical studies of contact of nominally flat surface; effect of previous loading", J. Lubrication Technology, Trans. ASME 451-459, 1971.

14. V.M. Popov, "Determination of the thermal contact resistance of plane-rough surfaces with roughness deforming in different manners", Heat Transfer - Soviet Research, vol. 2, no. 5, 26-31, 1970.

15. B.B. Mikic and G. Carnasciali, "The effect of thermal conductivity of plating material on thermal contact resistance", J. Heat Transfer, Trans. ASME 92, 475-483, 1970.

16. J. Dyson and W. Hirst, "The true contact area between solids", Proc. Physical Society, Sec. B, vol. 67, 309-312, 1954.

17. J.F. Archard, "Elastic deformation and the laws of friction", Proc. Roy. Soc. Lond. 243 A, 190, 1957.

18. I.V. Kragelsky and N.B. Demkin, "Contact area of rough surfaces, Wear 3", 170-187, 1960.

19. T. Tsukizoe and T. Hisakado, "On the mechanism of contact between metal surfaces - the penetrating depth and the average clearance", J. Basic Engineering, Trans. ASME, 666, 1965.

20. J.A. Greenwood, "Constriction resistance and the real area of contact", Brit. J. Appl. Phys. vol. 17, 1621-1632, 1966.

21. J.A. Greenwood and J.B.P. Williamson, "Contact of nominally flat surfaces", Proc. Roy. Soc. Lond. 295, 300-319, 1966.

22. J.A. Greenwood, "The area of contact between rough surfaces and flats", J. of Lubrication Technology, Trans. ASME, 81, 1967.

23. T. Tsukizoe and T. Hisakado, "On the mechanism of contact between metal surfaces: part 2 - the real area and the number of the contact points", J. of Lubrication Technology, Trans ASME, 81, 1968.

24. M.G. Cooper, B.B. Mikic and M.M. Yovanovich, "Thermal contact resistance, Int. J. Heat Mass Transfer, vol. 12, 279-300, 1969.

25. V.S. Novikov, "The thermal contact resistance as a function of compression of rough surfaces", Heat Transfer - Soviet Research, v 2 n 6, 160-165, 1970.

26. B.B. Mikic, "Thermal contact conductance, theoretical considerations", Int. J. Heat Mass Transfer, vol. 17, 205-214, 1974.

27. N. Vutz and S.W. Augrist, "Thermal contact resistance of anisotropic materials", J. of Heat Transfer, Trans ASME, 17, 1970.

28. M.M. Yovanovish, "Thermal contact conductance of turned surfaces", Prog. Astronant. Aeronaut. Fundam. of Spacecr, Therm. Des. v. 29 MIT Press, Cambridge, Mass. 289-305, 1972.

29. M.M. Yovanovich, "Thermal conductance of a raw of cylinders contacting two planes", Prog. Astronant, Aeronant., Fundam. of spacecr, Therm. Des. v. 29, MIT Press, Cambridge, Mass., 307-317, 1972.

30. T.R. Thomas and R.S. Sayles, "Random-process on thermal contact resistance", AIAA paper no. 74-691, 1974.

31. A. Williams, "Heat flows through single points of metallic contact of simple shapes", AIAA paper no. 74-692, 1974.

32. F.C. Yip, "The effect of oxide films on thermal contact resistance", AIAA paper no. 74-693, 1974.

33. M.M. Yovanovich and W.M. Rohsenow, "Influence of surface roughness and waviness upon thermal contact conductance", Technical Report no. 76361-48, Dept. of Mechanical Engineering, MIT, 1967.

34. Y.P. Shlykov and Y.A. Ganin, "Thermal resistance of metallic contacts", Int. J. Heat Mass Transfer 7, 921-929, 1964.

35. K. Sanokawa, "Heat transfer between metallic surfaces in contact", 3rd report, Bulletin of J.A.M.E. vol. 11, no. 44, 276-286, 1968.

36. G.F.C. Rogers, "Heat transfer at the interface dissimilar metals", Int. J. of Heat Mass Transfer 2, 150-154, 1961.

37. T.R. Thomas and S.D. Probert, "Thermal contact resistance: the direction effect and other problems", Int. J. Heat Mass Transfer 13, 789-807, 1970.

38. A. Williams, "Comments on the paper: Heat transfer at the interface of dissimilar metals - the influence of thermal strain", Int. J. Heat Mass Transfer 10, 1129-1130, 1967.

39. J.R. Barber, "Comments on the paper: Heat transfer at the interface of dissimilar metals - the influence of thermal strain", Int. J. Heat Mass Transfer 11, 617-618, 1968.

40. Joon Sang Moon and R.N. Keeler, "A theoretical consideration of directional effects in heat flow at the interface of dissimilar metals", Int. J. Heat Mass Transfer 5, 967-971, 1962.

41. P.D. Sanderson, "Heat transfer from uranium fuel to the magnox can in a gas-cooled reactor", 1961 International Heat Transfer Conference, Part 1, no. 8, Boulder, Colo., September, 1961.

42. A.C. Rapier, T.M. Jones and J.E. McIntosh, "Thermal conductance of uranium dioxide-stainless steel interfaces", Int. J. Heat Mass Transfer 6, 397-416, 1963.

43. A.M. Ross and R.L. Stoute, "Heat transfer coefficient between UO_2 and zircaloy-2", Report CRFD-1075, Atomic Energy of Canada Limited, 1962.

44. C.K. Hsieh, K.M. Yeddanapudi and Y.S. Touloukian, "An analytical study of thermal contact conductance for two rough and wavy surfaces under a pressure contact", U. S. Atomic Energy Commission 9th Conference on Thermal Conductivity, Oct. 6-8, 1969.

45. A.M. Clausing and B.T. Chao, "Thermal contact resistance in a vacuum environment", J. Heat Transfer 87, 243-251, 1965.

46. E. Volterra and J.H. Gaines, "Advanced Strength of Materials", Prentice-Hall, Inc., Englewood Cliffs, N.J., 1971.

47. E. Fried and F.A. Costello, "Interface thermal contact resistance problem in space vehicles", J. Am. Rock. Society 32, 237-243, 1962.

48. W.J. Graff, "Thermal conductance across metal joints", Machine Design, 166-172, 1960.

49. C.J. Moore and H.A. Blum, "Heat transfer across surfaces in contact: Effect of thermal transient on one-dimensional composite slabs", U. S. Bur. Standards - Special Publ. 302, Sept. 1968.

50. G.R. Horn, "The effects of xeon on fuel-to-cladding gap conductance", Trans. American Nuclear Society 12, 1969.

51. A.M. Abasov, "Solution of the fundamental linear nonideal contact-boundary problems for a composite cylinder", High Temperature, v. 9 n 1, 122-127, Jan.-Feb., 1971.

52. B. Mikic, "Thermal constriction resistance due to non-uniform surface conditions; contact resistance at non-uniform interface pressure", Int. J. Heat Mass Transfer, vol. 13, 1497-1500,1970.

53. S.S. Fengas, "Analogue study of thermal contact resistance for wavy and rough surfaces", M.Sc. Thesis, Mechanical Engineering Department, Massachusetts Institute of Technology, 1967.

54. J.J. Henry, "Thermal contact resistance", Sc. D. Thesis, Massachusetts Institute of Technology, 1964.

55. B. Mikic, "Thermal contact resistance", Sc. D. Thesis, Massachusetts Institute of Technology, 1967.

56. R. Holm, "Electric Contacts - Theory and Application", Springer-Verlag, New York Inc. 1967.

57. F.F. Ling, "Surface Mechanics", John Wiley & Sons, New York, 1973.

58. I.E. Campbell and E.M. Sherwood, "High Temperature Materials and Technology", John Wiley & Sons, Inc. New York, 1967.

59. D. Tabor, "The Hardness of Metals", Clarendon Press, Oxford, 1951.

60. C. Lipson and N.J. Sheth, "Statistical Design and Analysis of Engineering Experiments", McGraw-Hill Book Company, New York, 1973.

61. S.P. Timoshenko and J.N. Goodier, "Theory of Elasticity", McGraw-Hill Book Company, New York, 1951.

62. F.A. Disa, "Mechanics of Metals", Addison-Wesley Publishing Company, Inc. 1968.

63. M.E. Ozisik, "Boundary Value Problems of Heat Conduction", International Textbook Company, Pennsylvania, 1968.

64. S.J. Kline and F.A. McClintock, "Describing uncertainty in single-sample experiments", Mechanical Engineering Journal, 3-8, January, 1953.

Appendix A Error Analysis of Experiment

Statistics is considered to be a powerful tool of analyzing the errors in experimental results. In this experiment, because of insufficient observations, the reliability of the results could not be assured by the use of statistics, however, an error analysis based on a single-sample experiments suggested by Kline and McClintock [64] was used for the subsequent analysis.

Using their terminologies and notations, the uncertainty in each variable was defined by the mean of the readings and an uncertainty interval based on specified odds. Therefore

$$m \pm \omega, \text{ (b to 1)} \tag{A1}$$

where m = arithmatic mean of the observed values

ω = uncertainty interval

b = odds

The result R was defined as a function of n independent variables, v_1, v_2, ..., v_n.

$$R = R\ (V_1, V_2, \ldots, V_n) \tag{A2}$$

The uncertainties in the variables V_i are described by uncertainty intervals ω_i based on certain odds. The uncertainty for the result, ω_R, which gives the same odds for each of the variables and for the result is related to the uncertainty intervals for the variables by a second-power equation as follows:

$$\omega_R = [(\frac{\partial R}{\partial V_1}\omega_1)^2 + (\frac{\partial R}{\partial V_2}\omega_2)^2 + \ldots. + (\frac{\partial R}{\partial V_n}\omega_n)^2]^{1/2} \tag{A3}$$

For this error analysis, twenty to one were taken for each of the variables.

Method

Thermal contact resistance is defined by Eq. 1 as follows:

$$R_c = \frac{\Delta T_c}{(Q/A_a)}$$

Since $$A_a = 2\pi \gamma_2 \ell$$

it becomes $$R_c = \frac{2\pi \gamma_2 \ell \ \Delta T_c}{Q} \qquad (A4)$$

Equation A4 was used to determine the uncertainty interval for the thermal contact resistance due to the variables, ℓ, γ_2, ΔT_c, and Q. That is:

$$\omega_{R_c} = [(\frac{\partial R_c}{\partial \ell} \omega_\ell)^2 + (\frac{\partial R_c}{\partial \tau_2} \omega_{r_2})^2 + (\frac{\partial R_c}{\partial \Delta T_c} \omega_{\Delta T_c})^2 + (\frac{\partial R_c}{\partial Q} \omega_Q)^2]^{1/2} \qquad (A5)$$

To simplify Eq. (A5), differentiation was performed and Eq. (A5) was divided by Eq. (A4) to yield:

$$\frac{\omega_{R_c}}{R_c} = [(\frac{\omega_\ell}{\ell})^2 + (\frac{\omega_{r_2}}{\gamma_2})^2 + (\frac{\omega_{\Delta T_c}}{\Delta T_c})^2 + (\frac{\omega_Q}{Q})^2]^{1/2} \qquad (A6)$$

Sample Calculation

The following calculation was performed for test 1.1, from which the worst error in thermal contact resistance occured. The test had the following mean values and uncertainty intervals:

$\ell = 5.680 \pm 0.005$ (inches)

$\gamma_2 = 1.1645 + 0.001$ (inches)

$\Delta T_c = 0.3595 \pm 0.005$ (^oF)

$Q = 0.1472 + 0.0074$ (Btu/sec)

Substituting the above values into Eq. A6, the percentage uncertainty in thermal contact resistance was:

$$\frac{\omega_{R_c}}{R_c} = [(7.75 \times 10^{-7}) + (7.37 \times 10^{-7}) + (1.93 \times 10^{-4}) + (2.53 \times 10^{-3})]^{1/2}$$

$$= \pm 5.22\%$$

APPENDIX B

DERIVATION OF PRE-CONTACT PRESSURE AND THERMAL CONTACT PRESSURE

B(1) Pre-contact Pressure

In order to study the pre-contact pressure of a shunk fit composite cylinder, let us consider two cylinders, 1 and 2 (see Fig. 43). The radial displacement of a thick wall cylinder subjected to external and internal pressures is given as (46):

$$u = \frac{1-\nu}{E} \cdot \frac{P_o r_o^2 - P_i r_i^2}{r_o^2 - r_i^2} \cdot r + \frac{1+\nu}{E} \cdot (P_o - P_i) \cdot \frac{r_o^2 r_i^2}{r_o^2 - r_i^2} \cdot \frac{1}{r} \qquad \text{(B1)}$$

If, in Eq. (B1), $P_i = P_{sc} \neq 0$, $P_o = 0$, $r_o = r_3$ and $r_i = r_2$, the deformation (U_{c2}) at the inside of cylinder 2 (for $r=r_2$) will be:

$$u_{c2} = - \frac{P_{sc}\, r_2}{E_2} \cdot \left(\frac{r_3^2 + r_2^2}{r_3^2 - r_2^2} + \nu_2\right) \qquad \text{(B2)}$$

If, in Eq. (B1), $P_i = 0$, $P_o = P_{sc} \neq 0$, $r_o = r_2$ and $r_i = r_i$, the deformation (U_{c1}) at the outside of cylinder 1 (for $r=r_2$) will be:

$$u_{c1} = \frac{P_{sc}\, r_2}{E_1} \cdot \left(\frac{r_2^2 + r_1^2}{r_2^2 - r_1^2} - \nu_1\right) \qquad \text{(B3)}$$

For the case of two cylinders shrunk together, the interference of metal is $\delta = 2 \cdot (|U_{c1}| + |U_{c2}|)$. Then from (B2) and (B3) one obtains

$$\frac{P_{sc}\, r_2}{E_2} \cdot \left(\frac{r_3^2 + r_2^2}{r_3^2 - r_2^2} + \nu_2\right) + \frac{P_{sc}\, r_2}{E_1} \cdot \left(\frac{r_2^2 + r_1^2}{r_2^2 - r_1^2} - \nu_1\right) = \frac{\delta}{2}$$

from which

$$P_{sc} = \frac{\frac{\delta}{2}}{r_2\left[\frac{1}{E_1}\left(\frac{r_2^2 + r_1^2}{r_2^2 - r_1^2} - \nu_1\right) + \frac{1}{E_2}\left(\frac{r_3^2 + r_2^2}{r_3^2 - r_2^2} + \nu_2\right)\right]} \qquad \text{(B4)}$$

B(2) Thermal Contact Pressure

Considering a long hollow cylinder subjected to a radial temperature distribution, the differential equation of displacement for a plane-strain case is:

$$\frac{d}{dr}\left[\frac{1}{r}\frac{d(ru)}{dr}\right] = \frac{1+\nu}{1-\nu}\alpha\frac{dT}{dr} \tag{B5}$$

The general solution is:

$$u(r) = \frac{1+\nu}{1-\nu}\frac{\alpha}{r}\int_{r_1}^{r} T(r)\, rdr + Ar + \frac{B}{r} \tag{B6}$$

From the strain-displacement equations and the Hooke's law the thermal stresses are given as:

$$\sigma_{rr} = -\frac{\alpha E}{1-\nu}\cdot\frac{1}{r_2}\cdot\int_{r_1}^{r} T(r)dr + \frac{E}{1+\nu}\left(\frac{A}{1-2\nu} - \frac{B}{r^2}\right)$$

$$\sigma_{\theta\theta} = \frac{\alpha E}{1-\nu}\cdot\frac{1}{r^2}\cdot\int_{r_1}^{r_2} T(r)rdr - \frac{\alpha E T(r)}{1-\nu} + \frac{E}{1+\nu}\left(\frac{A}{1-2\nu} + \frac{B}{r^2}\right) \tag{B7}$$

$$\sigma_{zz} = -\frac{\alpha E\, T(r)}{1-\nu} + \frac{2\nu E A}{(1+\nu)(1-2\nu)}$$

where A and B are arbitrary constants determined by the boundary conditions.

Now, in determining the thermal stresses of a composite cylinder, the problem is then defined by the following:

$$u_1 = \frac{1+\nu_1}{1-\nu_1}\cdot\frac{\alpha_1}{r}\cdot\int_{r_1}^{r} T_1(r)rdr + Ar + \frac{B}{r}$$

$$\sigma_{rr_1} = -\frac{\alpha_1 E_1}{1-\nu_1}\cdot\frac{1}{r^2}\cdot\int_{r_1}^{r} T_1(r)rdr + \frac{E_1}{1+\nu_1}\left(\frac{A}{1-2\nu_1} - \frac{B}{r^2}\right)$$

$$\sigma_{\theta\theta_1} = \frac{\alpha_1 E_1}{1-\nu_1} \cdot \frac{1}{r^2} \cdot \int_{r_1}^{r} T_1(r) r dr - \frac{\alpha_1 E_1 T_1(r)}{1-\nu_1} + \frac{E_1}{1+\nu_1} \left(\frac{A}{1-2\nu_1} + \frac{B}{r^2}\right) \quad \text{(B8)}$$

$$\sigma_{zz_1} = - \frac{\alpha_1 E_1 T_1(r)}{1-\nu_1} + \frac{2\,\nu_1\, E_1\, A}{(1+\nu_1)(1-2\nu_1)}$$

in cylinder 1,

and

$$u_2 = \frac{1+\nu_2}{1-\nu_2} \cdot \frac{\alpha_2}{r} \cdot \int_{r_2}^{r} T_2(r) r dr + Dr + \frac{F}{r}$$

$$\sigma_{rr_2} = - \frac{\alpha_2 E_2}{1-\nu_2} \cdot \frac{1}{r^2} \cdot \int_{r_2}^{r} T_2(r) r dr + \frac{E_2}{1+\nu_2} \left(\frac{D}{1-2\nu_2} - \frac{F}{r^2}\right)$$

$$\sigma_{\theta\theta_2} = \frac{\alpha_2 E_2}{1-\nu_2} \cdot \frac{1}{r^2} \cdot \int_{r_2}^{r} T_2(r) r dr - \frac{\alpha_2 E_2 T_2(r)}{1-\nu_2} + \frac{E_2}{1+\nu_2} \cdot \left(\frac{D}{1-2\nu_2} + \frac{F}{r^2}\right) \quad \text{(B9)}$$

$$\sigma_{zz_2} = - \frac{\alpha_2 E_2 T_2(r)}{1-\nu_2} + \frac{2\nu_2 E_2 D}{(1+\nu_2)(1-2\nu_2)}$$

in cylinder 2.

The boundary conditions are given as:

$$\begin{aligned} \sigma_{rr_1} &= 0 && \text{at } r = r_1 \\ \sigma_{rr_1} &= \sigma_{rr_2} && \text{at } r = r_2 \\ u_1 &= u_2 && \text{at } r = r_2 \\ \sigma_{rr_2} &= 0 && \text{at } r = r_3 \end{aligned} \quad \text{(B10)}$$

Defining for convenience,

$$e_1 = \frac{E_1}{1-\nu_1} \qquad e_4 = \frac{E_2}{1-\nu_2}$$

$$e_2 = \frac{E_1}{1+\nu_1} \qquad e_5 = \frac{E_2}{1+\nu_2}$$

$$e_3 = \frac{1}{1-2\nu_1} \qquad e_6 = \frac{1}{1-2\nu_2} \tag{B11}$$

$$h_1 = \int_{r_1}^{r_2} T_1(r) r dr \qquad h_2 = \int_{r_2}^{r_3} T_2(r) r\, dr$$

From the boundary conditions, the arbitrary constants, A, B, D and F are determined by:

$$A = \frac{(g-1)e_1\alpha_1 h_1 + (g-\frac{e_2}{e_5})e_4\alpha_2 h_2}{e_2[r_2^2(ge_3+1) + e_3 r_1^2(1-g)]}$$

$$B = e_3\, r_1^2\, A$$

$$D = \frac{-e_2e_3(r_2^2-r_1^2)A + e_1\alpha_1 h_1 + e_4\alpha_2 h_2}{e_5e_6(r_3^2-r_2^2)} \tag{B12}$$

$$F = \frac{e_5e_7r_3^2\, D - e_4\alpha_2 h_2}{e_5}$$

where

$$g = \frac{e_2(r_2^2 + e_6\, r_3^2)}{e_5e_6(r_3^2 - r_2^2)}$$

Hence the deformation and the thermal stresses of a composite cylinder can be completely defined by Eqs. (B8), (B9), (B11) and (B12).

The thermal contact pressure is equal to the radial stress component at the contacting interface, and it can be either obtained from Eqs. (B8) or Eq. (B9) by putting $r = r_2$.

Letting:

$$P_c = \sigma_{rr_1} (r = r_2) = \sigma_{rr_2} (r = r_2)$$

it yields

$$P_c = \frac{e_2 e_3 A(r_2^2 - r_1^2) - e_1 \alpha_1 h_1}{r_2^2} \tag{B13}$$

or

$$P_c = \frac{e_4 \alpha_2 h_2 - e_5 e_6 D(r_3^2 - r_2^2)}{r_2^2} \tag{B14}$$

TABLE 1

Mechanical and Physical Properties of 2011-T351 Alclad

Mechanical Properties

Ultimate Strength Ksi	Yield Strength Ksi	Modulus of Elasticity 10^6 psi	Microhardness Ksi
50	43	10.3	135

Physical Properties

Density lb/in^3	Melting Range F	Thermal Conductivity Btu/hr-ft- F	Coefficient of Linear Expansion / F 10^{-6}
0.102	995 - 1193	89.51	12.67

TABLE 2

Mechanical and Physical Properties of 304 Stainless Steel

Mechanical Properties

Ultimate Strength Ksi	Yield Strength Ksi	Modulus of Elasticity 10^6 psi	Microhardness Ksi
75 - 100	30 - 60	29	350

Physical Properties

Density lb/in^3	Melting Range F	Thermal Conductivity Btu/hr-ft- F	Coefficient of Linear Expansion / F 10^{-6}
0.28	2550 - 2590	9.42	9.6

TABLE 3

Test Schedule and Description of Specimen

Test	2011-T351 Alclad			304 Stainless Steel			Interfacial
	I. D. in.	O. D. in.	Surface Roughness microin. rms	I. D. in.	O. D. in.	Surface Roughness microin. rms	Gas
TCR - 1	0.875	$2.329^{+.001}_{-.000}$	120 - 190	2.329	2.855	50 - 65	Air
TCR - 2	0.875	$2.329^{+.001}_{-.000}$	30 - 37	2.329	2.852	50 - 65	Air
TCR - 2.XR	Same test specimen as TCR - 2.						

TABLE 4

Test Results

(1) TCR - 1

Test No.	Q/A_a Btu/sec-in^2-^oF x 10^3	P_c psi	ΔT_c ^oF	T_c ^oF	k_{air} Btu/hr-in-^oF	R_c sec-in^2-^oF/Btu	R_c M. Ross & Stoute sec-in^2-^oF/Btu	R_c Shlykov & Ganin sec-in^2-^oF/Btu
1.1	3.54	2800	0.36	61.74	0.0146	101.86	177.94	139.02
1.2	6.47	3100	0.75	67.56	0.0147	116.90	170.45	131.88
1.3	13.24	3500	1.01	75.45	0.0149	76.10	159.00	121.13
1.4	17.48	3800	1.22	80.03	0.0159	70.06	152.65	115.32
1.5	20.49	4100	1.34	85.53	0.0151	65.45	147.51	110.72
1.6	27.00	4500	1.69	93.38	0.0153	62.75	138.93	103.12

TABLE 4

(continued)

Test Results

(2) TCR - 2

Test No.	Q/A_a Btu/sec-in^2-^{o}F x 10^3	P_c psi	ΔT_c ^{o}F	T_c ^{o}F	k_{air} Btu/hr-ft-^{o}F	R_c sec-in^2-^{o}F/Btu	R_c M. Ross & Stoute sec-in^2-^{o}F/Btu	R_c Shlykov & Ganin sec-in^2-^{o}F/Btu
2.1	8.2	3300	0.59	76.10	0.0149	72.00	82.95	81.62
2.2	10.45	3500	0.68	81.72	0.0150	65.41	80.76	79.43
2.3	13.20	3800	0.82	89.95	0.0152	62.14	77.84	76.50
2.4	15.54	4000	0.90	97.01	0.0153	57.70	75.55	74.21
2.5	17.37	4200	0.97	102.18	0.0154	55.58	73.91	75.57
2.6	19.41	4400	1.00	108.28		51.40	72.14	70.80

TABLE 4

(continued)

Test Results

(3) TCR - 2.XR

Test No.	Q/A_a Btu/sec-in^2-^oF x 10^3	P_c psi	ΔT_c ^oF	T_c ^oF	k_{air} Btu/hr-ft-^oF	R_c sec-in^2-^oF/Btu	R_c M. Ross & Stoute sec-in^2-^oF/Btu	R_c Shlykov & Ganin sec-in^2-^oF/Btu
2.1R	11.75	3600	0.74	83.84	0.0151	63.32	79.73	78.38
2.2R	14.04	3800	0.83	91.39	0.0152	59.22	77.23	75.90
2.3R	16.61	4100	0.94	100.01	0.0154	56.77	74.59	73.25
2.4R	18.00	4200	0.97	102.63	0.0155	54.11	73.63	72.29
2.5R	19.05	4300	0.99	104.85	0.0155	52.06	72.88	71.54
2.6R	20.08	4500	1.03	111.74	0.0156	51.16	71.31	69.98

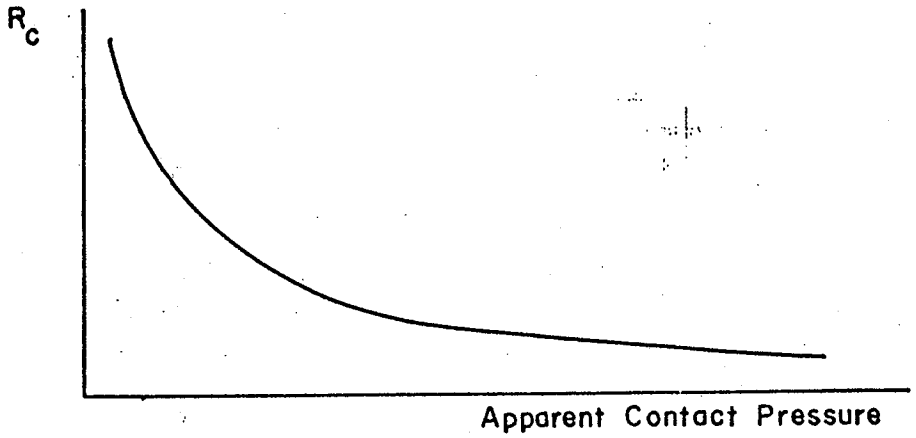

Fig. 1 Effect of Apparent Contact Pressure on Thermal Contact Resistance

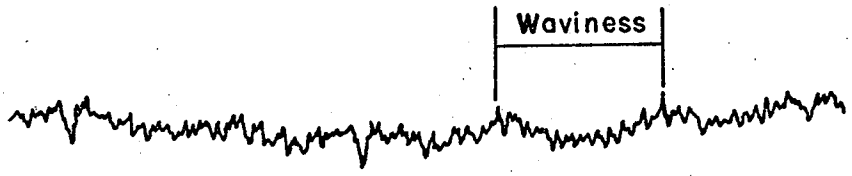

Fig. 2 Typical Surface Profile Showing Surface Roughness and Waviness

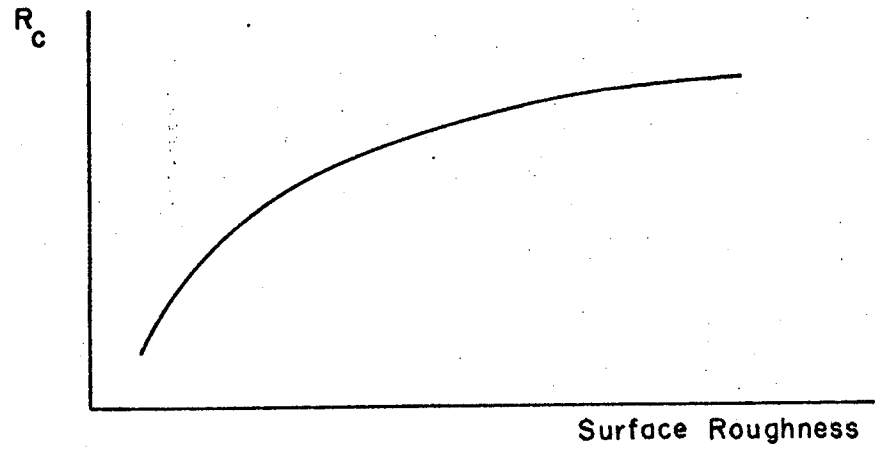

Fig. 3 Effect of Surface Roughness on Thermal Contact Resistance

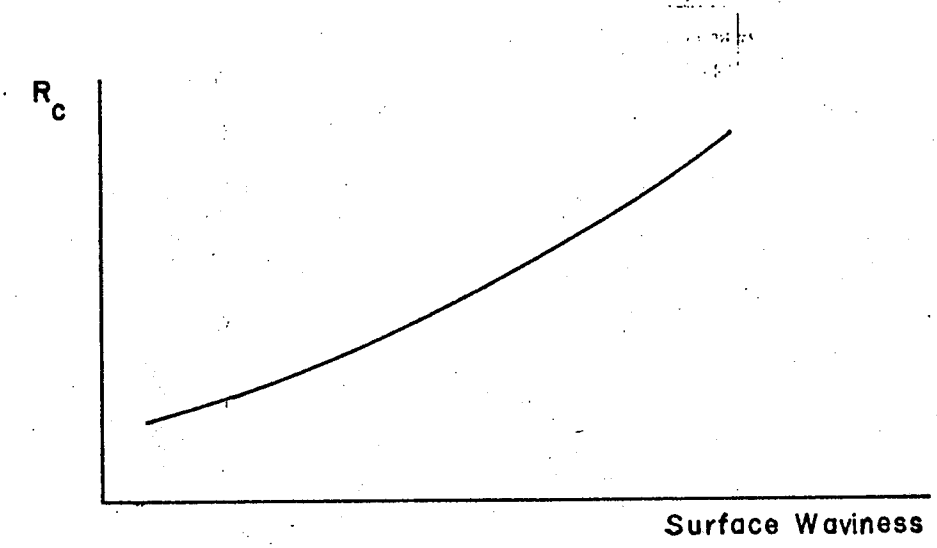

Fig. 4 Effect of Surface Waviness on Thermal Contact Resistance

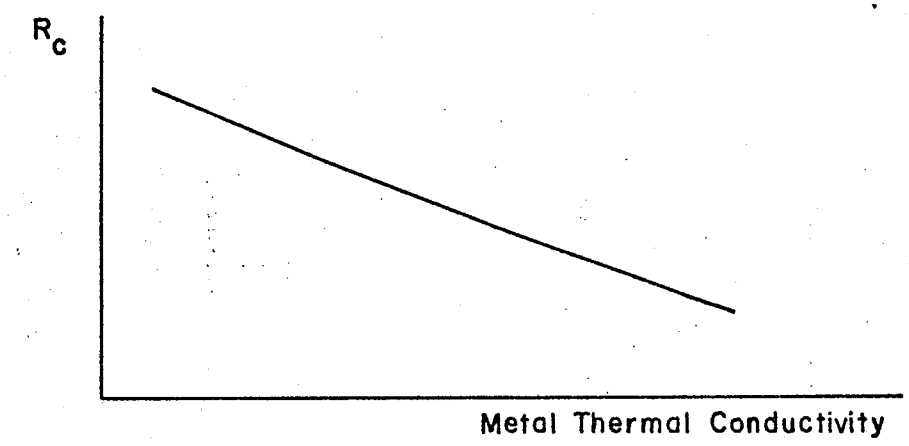

Fig. 5 Dependence of Thermal Contact Resistance on Metal Thermal Conductivity

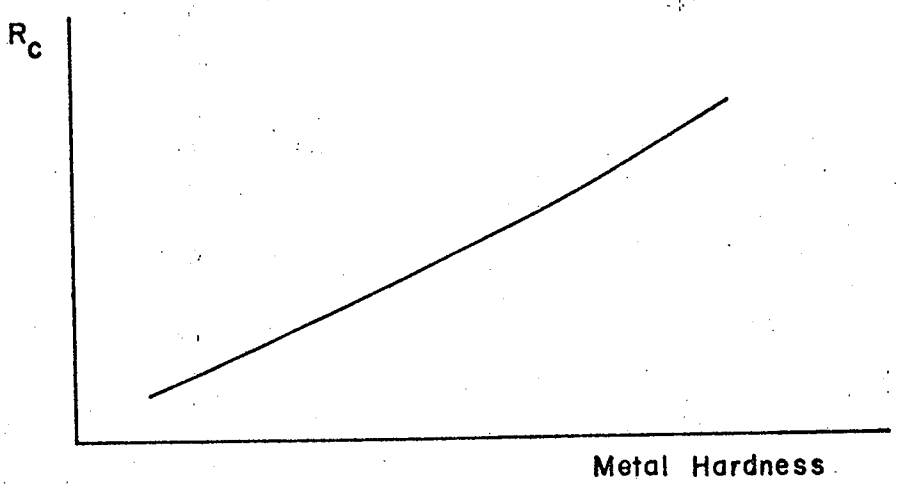

Fig. 6 Dependence of Thermal Contact Resistance on Metal Hardness

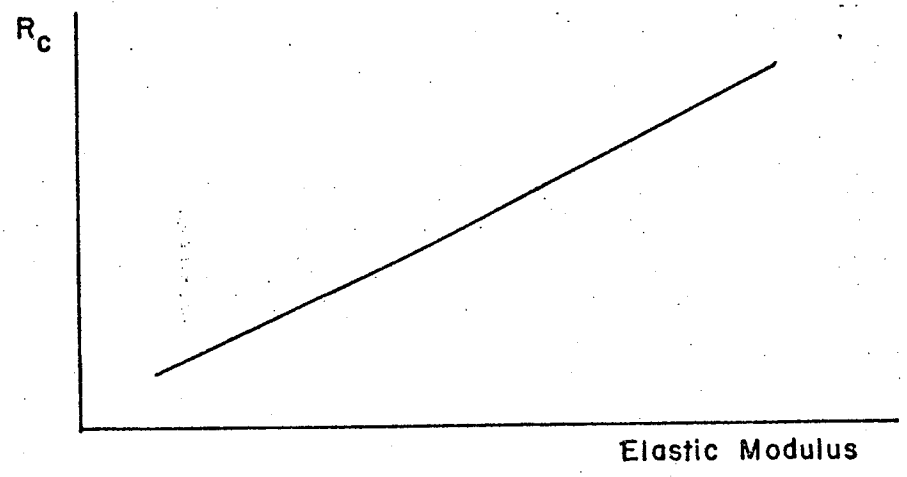

Fig. 7 Dependence of Thermal Contact Resistance on Elastic Modulus

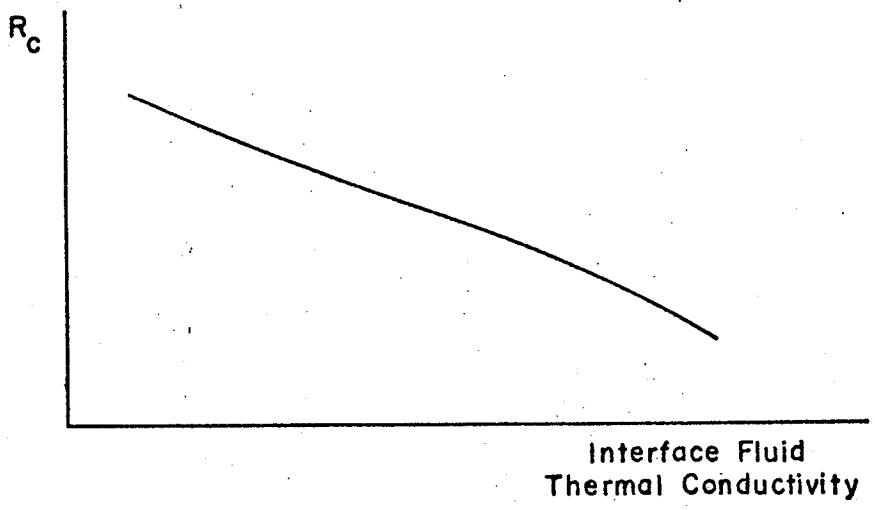

Fig. 8 Dependence of Thermal Contact Resistance on Interfacial Fluid Thermal Conductivity

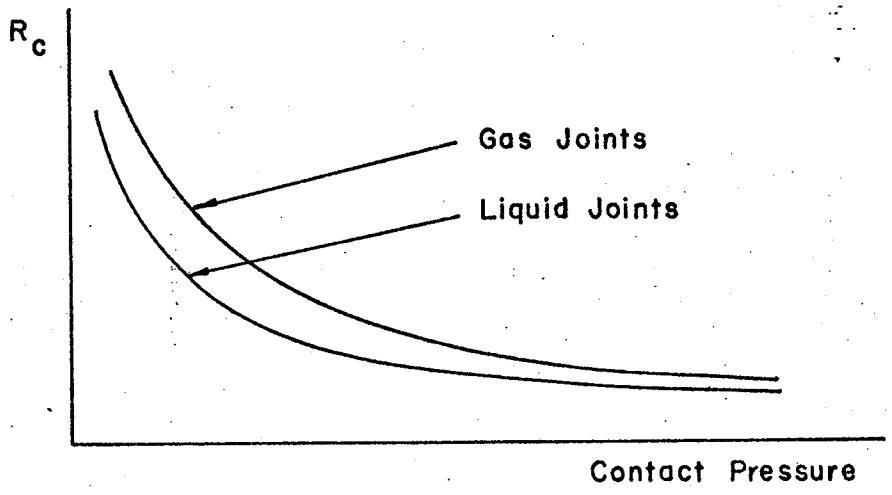

Fig. 9 Influence of Interfacial Fluid on Thermal Contact Resistance

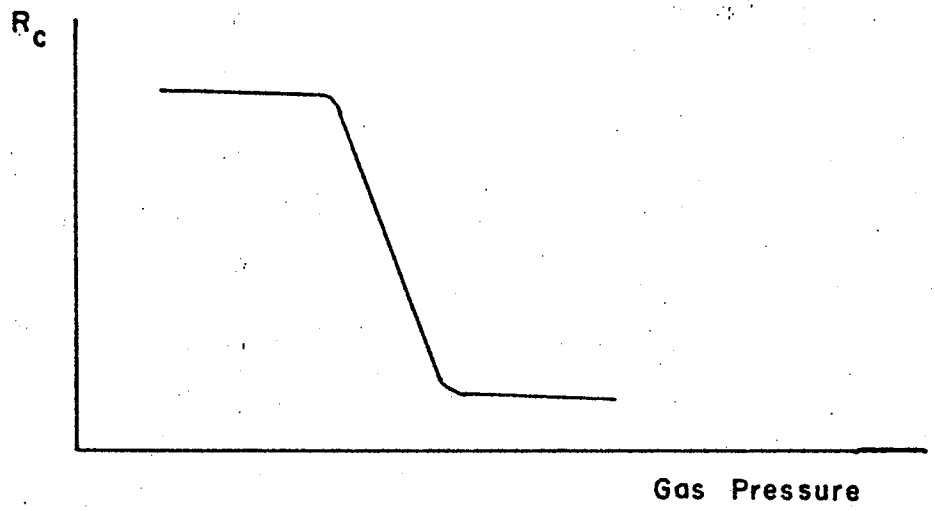

Fig. 10 Influence of Interfacial Gas Pressure on Thermal Contact Resistance

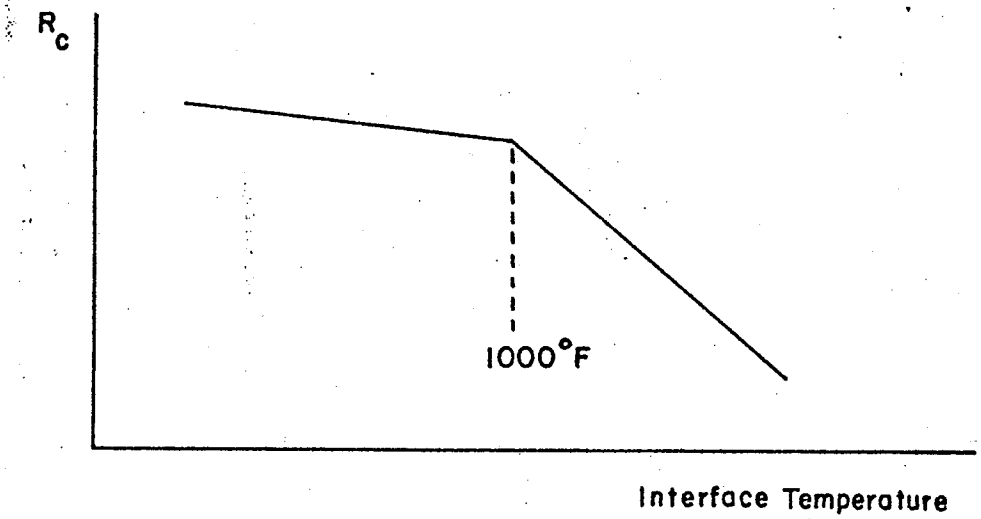

Fig. 11 Dependence of Thermal Contact Resistance on Mean Interface Temperature

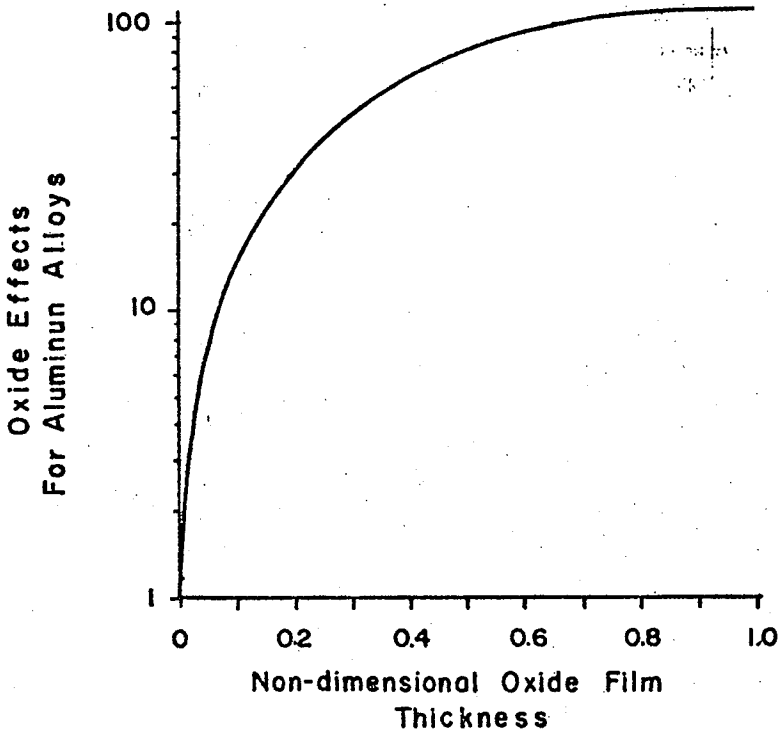

Fig. 12 Effect of Aluminum Oxide Film Thickness on Thermal Contact Resistance [32]

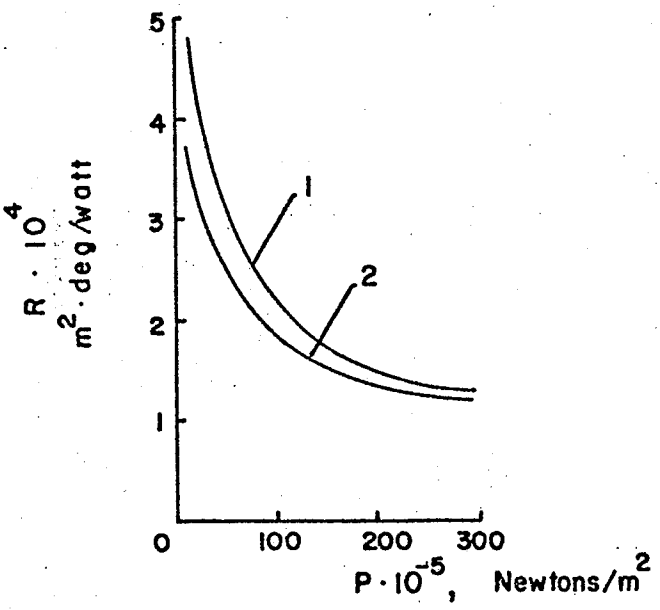

Fig. 13 Variation of Thermal Contact Resistance on Loading Conditions. Curves1 and 2 are for initial and Subsequent load applications respectively [25]

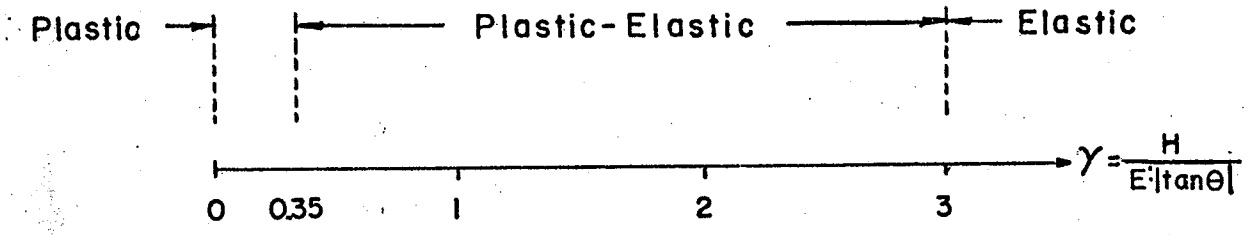

Fig. 14 Schematic Representation of Mode of Deformation of Surface Asperities

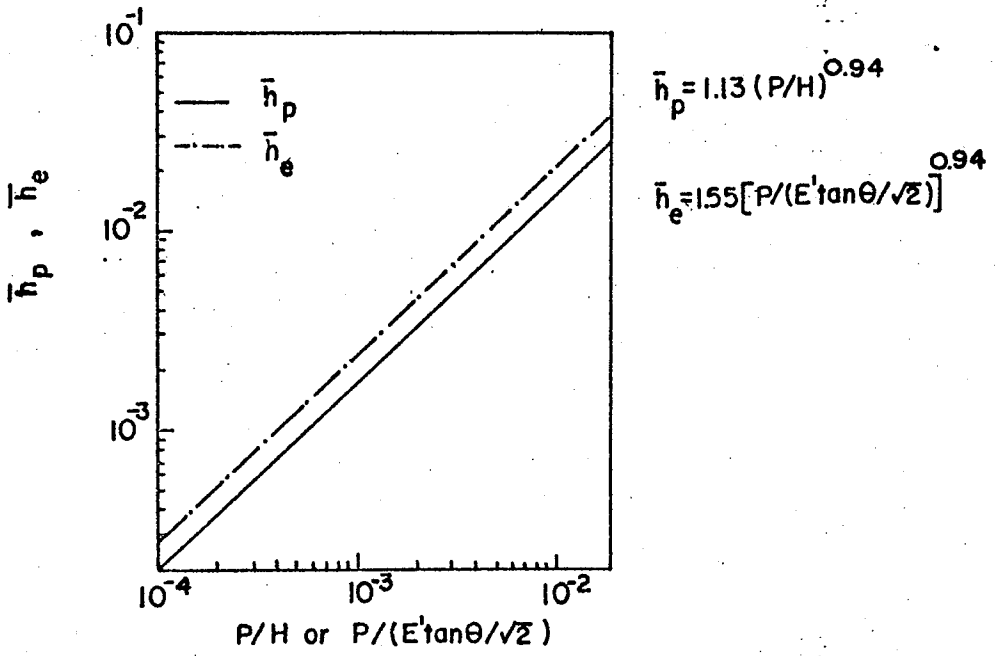

Fig. 15 Thermal Contact Conductance vs Interface Pressure for Elastic [h_e] and Plastic [h_p] of Asperities [26]

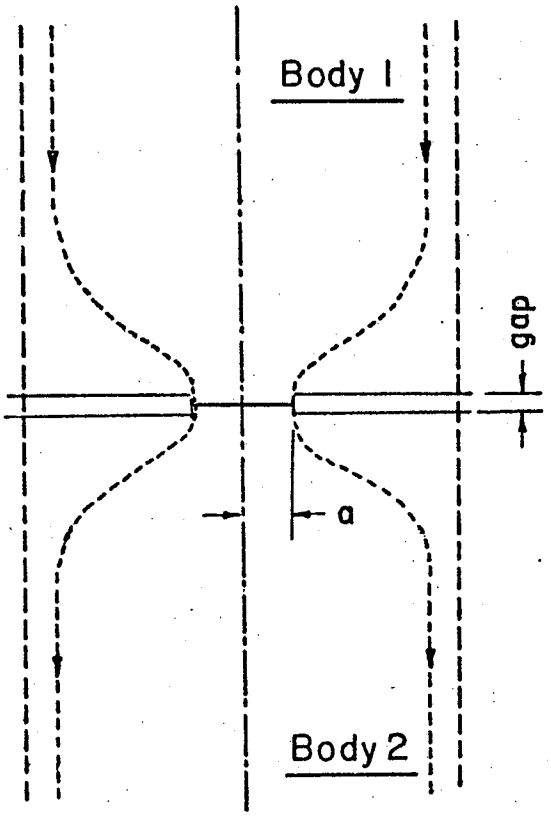

Fig. 16 Conventional Idealized Contact Model

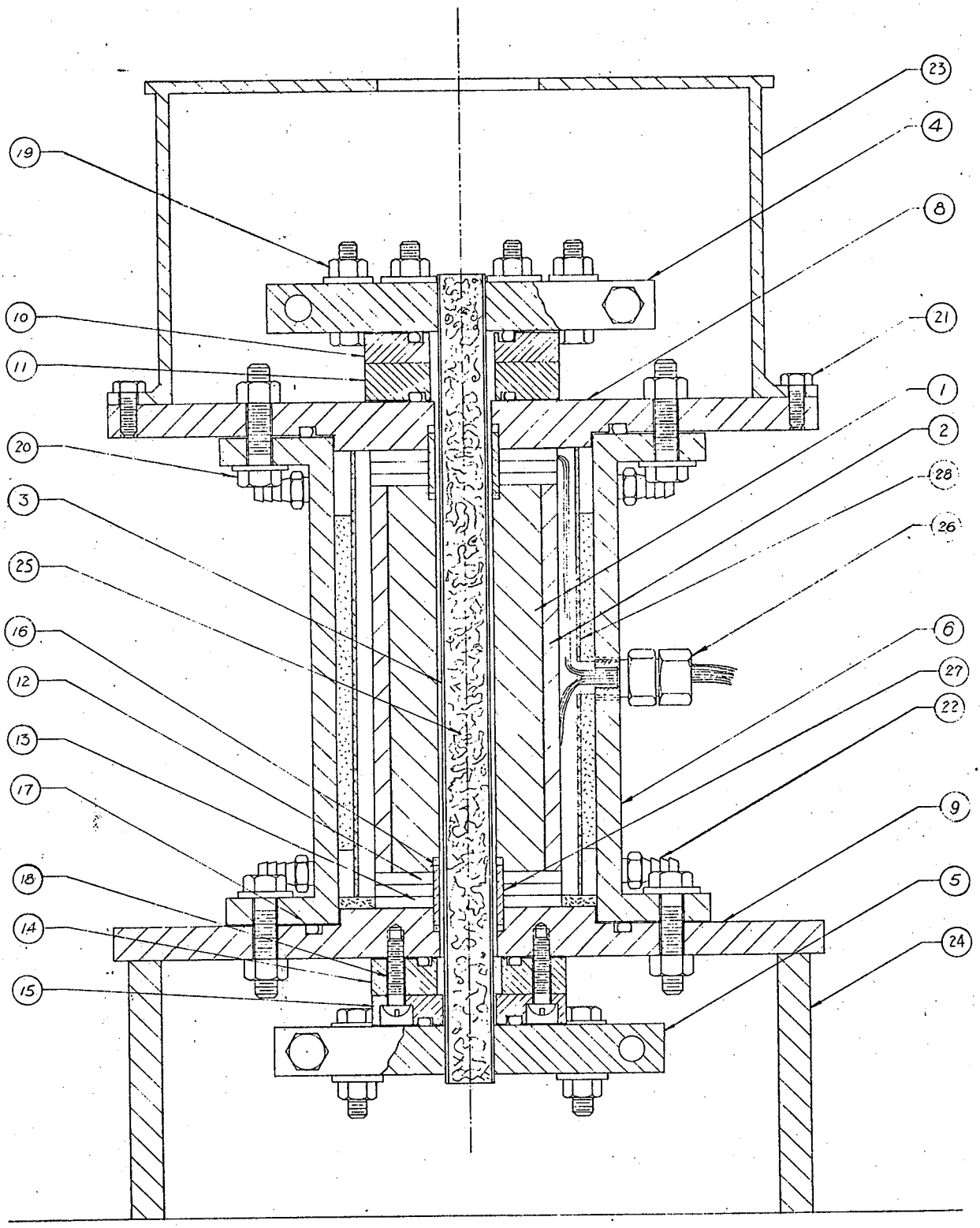

Fig. 17 Test Apparatus

Description of Designed Parts

NO.	Description
1	Aluminum test cylinder
2	Stainless steel test cylinder
3	Heating element
4 , 5	Power terminal
6	Steel shell
8 , 9	Base plate
10 , 15	Asbestos flange
11 , 14	Steel flange
12	Teflon guard ring
16	Teflon seal
17	O-ring
25	Insulation
26	Conax seal
27	Centering bushing
28	Close-up water jacket

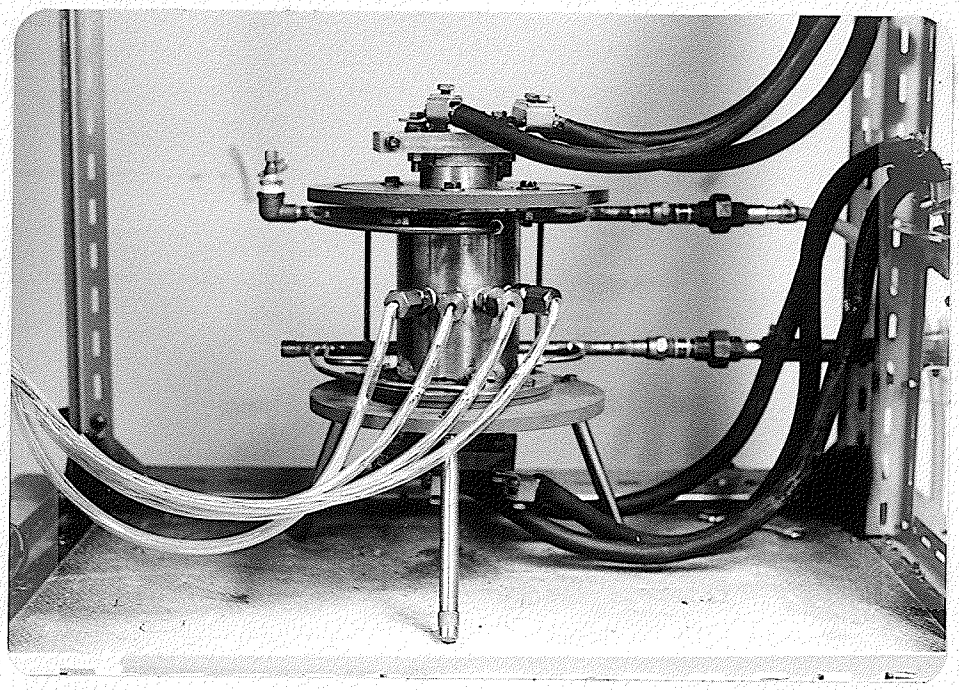

Fig. 18 Close-up View of Test Rig

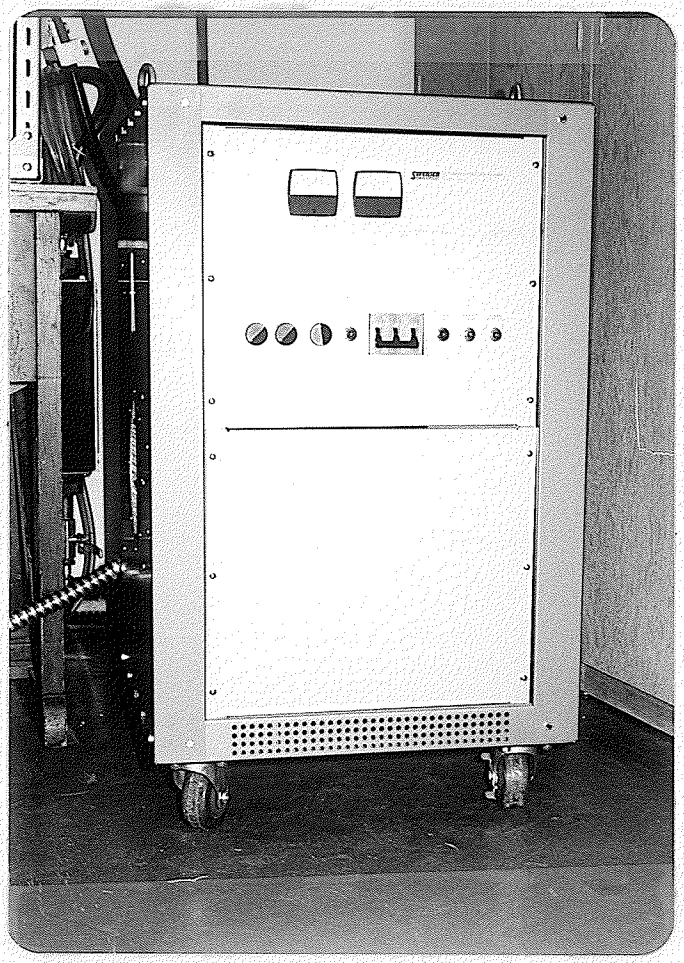

Fig. 19 Three Phase Input DC Power Supply

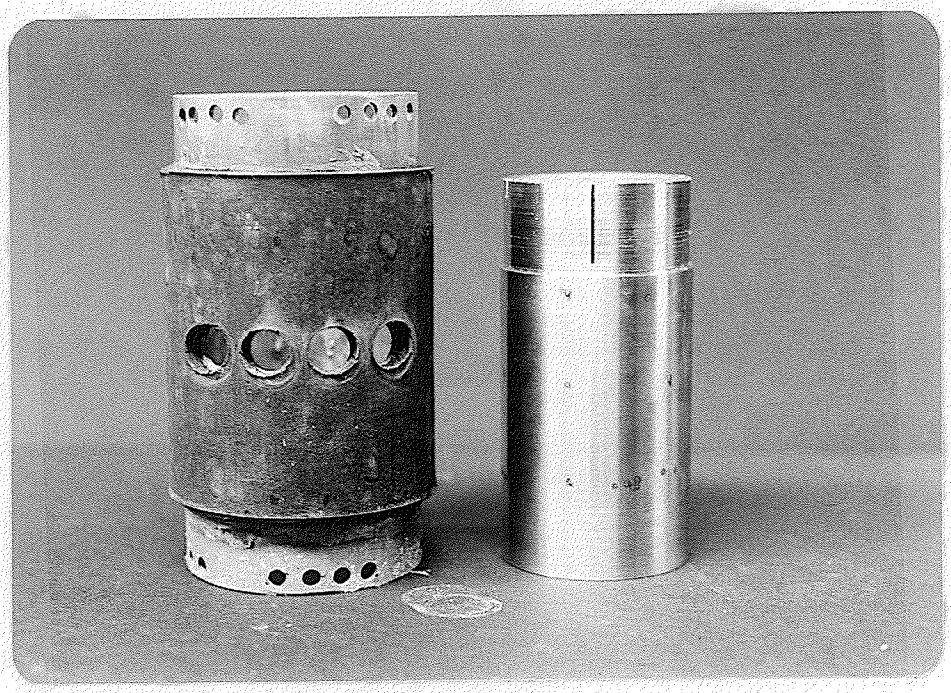

Fig. 20 Close-up Water Jacket and Dummy Specimen

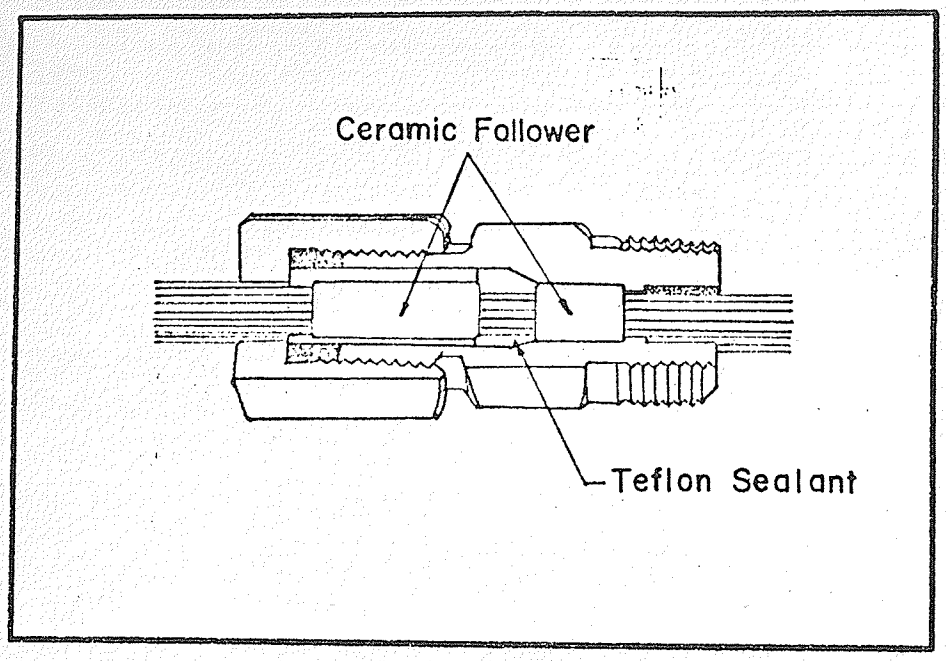

Fig. 21 Sketch of Conax Seal

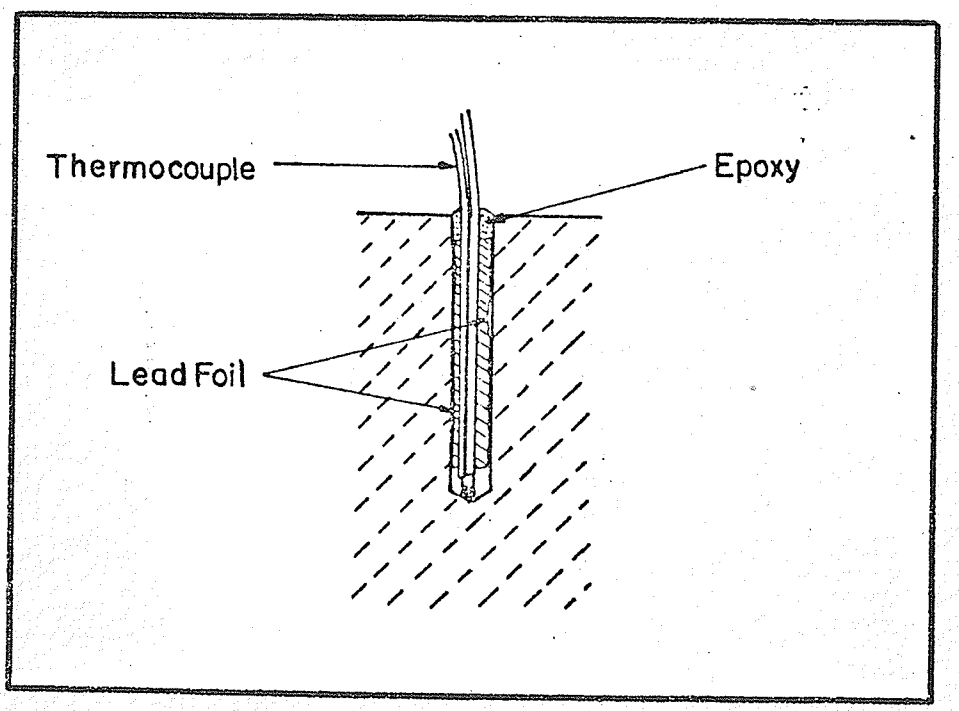

Fig. 22 Section View of Thermocouple Installation

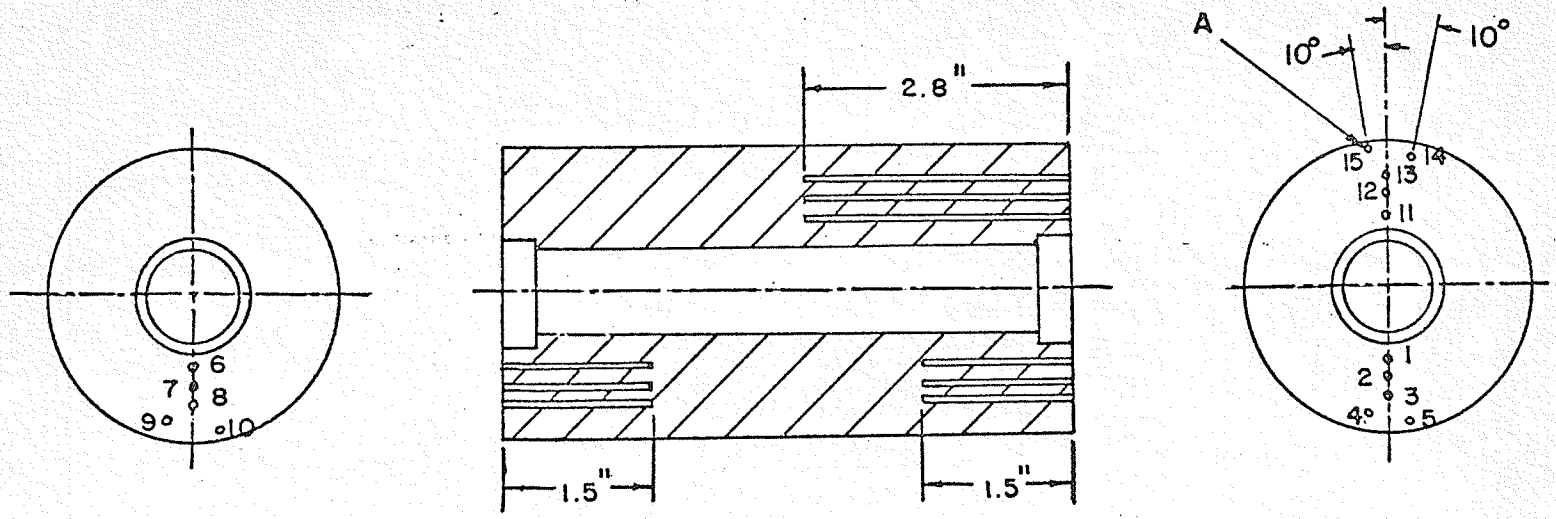

Legend: A — 1/16 " dia. drilled hole

Radial Dist.(in.)	0.6875	0.875	1.0625	1.27	1.35
Upper Level	1	2	3	4	5
Lower Level	6	7	8	9	10
Mid Level	11	12	13	14	15

Fig. 23 Location of Thermocouple Wells for Specimen TCR-1

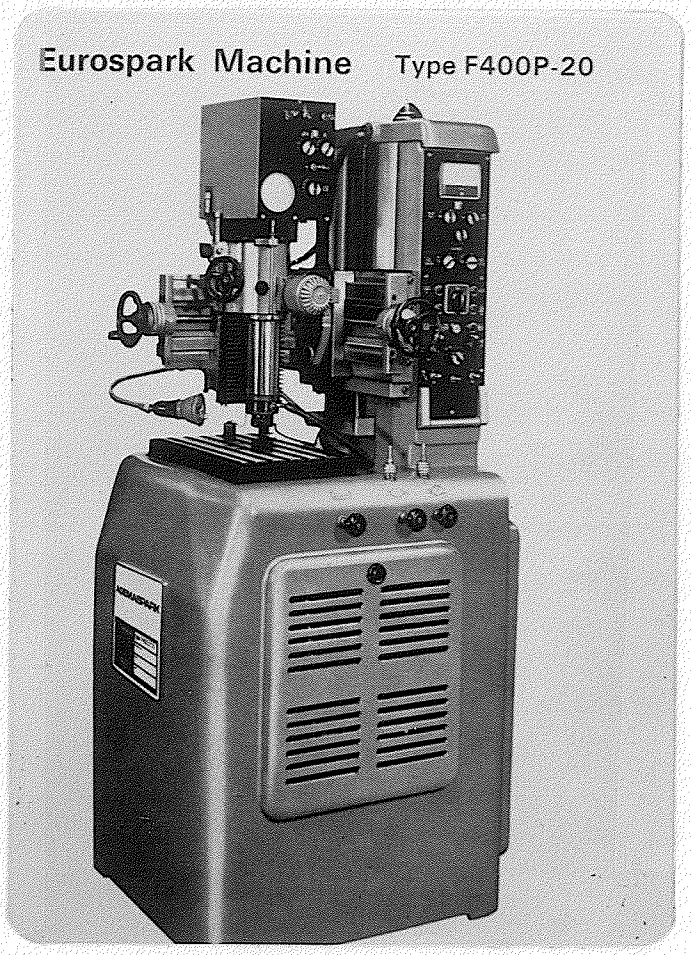

Fig. 24 General View of Eurospark Machine

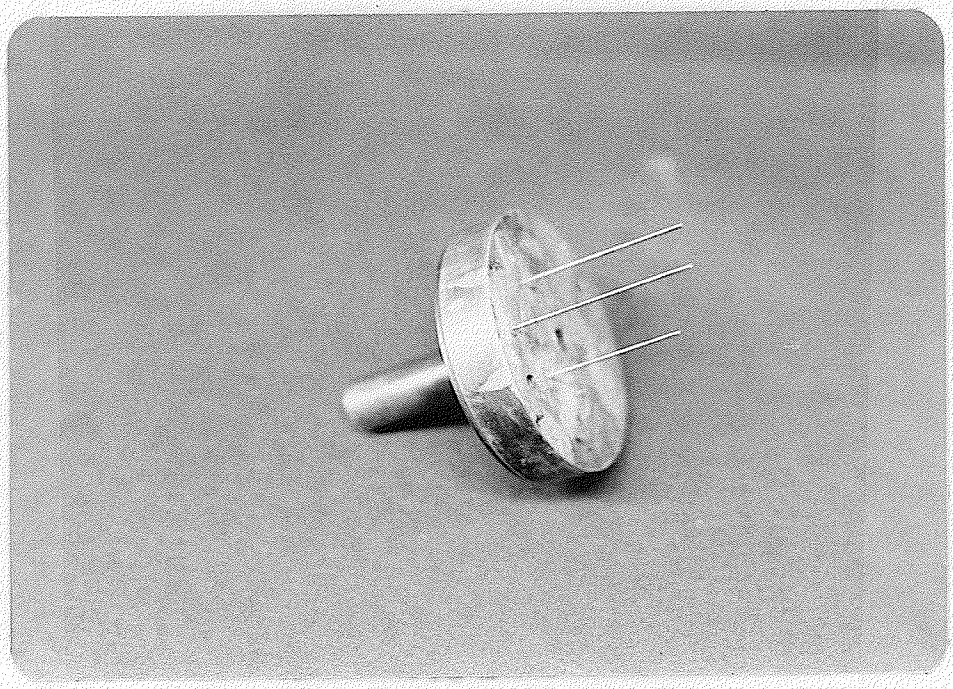

Fig. 25 Multi-element Tool Holder

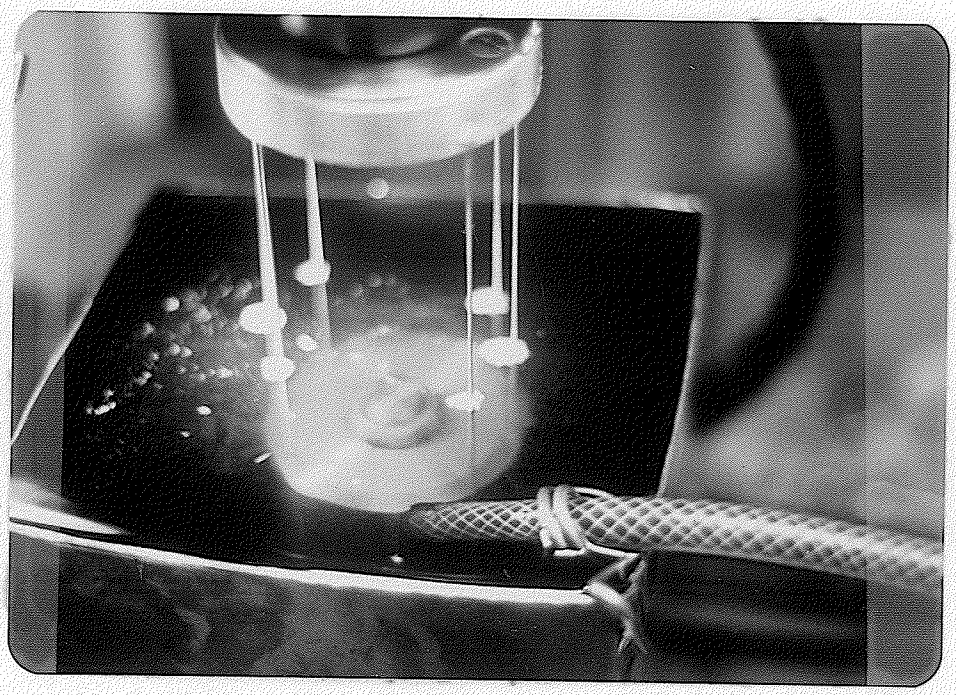

Fig. 26 Photograph of Specimen TCR-2 during Drilling

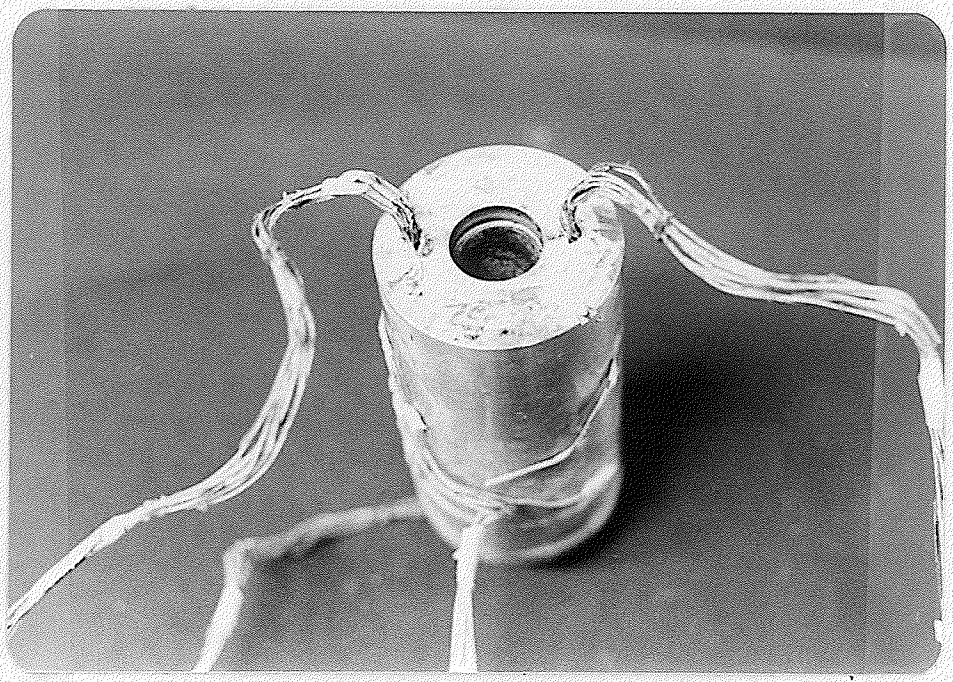

Fig. 27 Test Specimen TCR-2 Showing Embedded Thermocouple Bundles

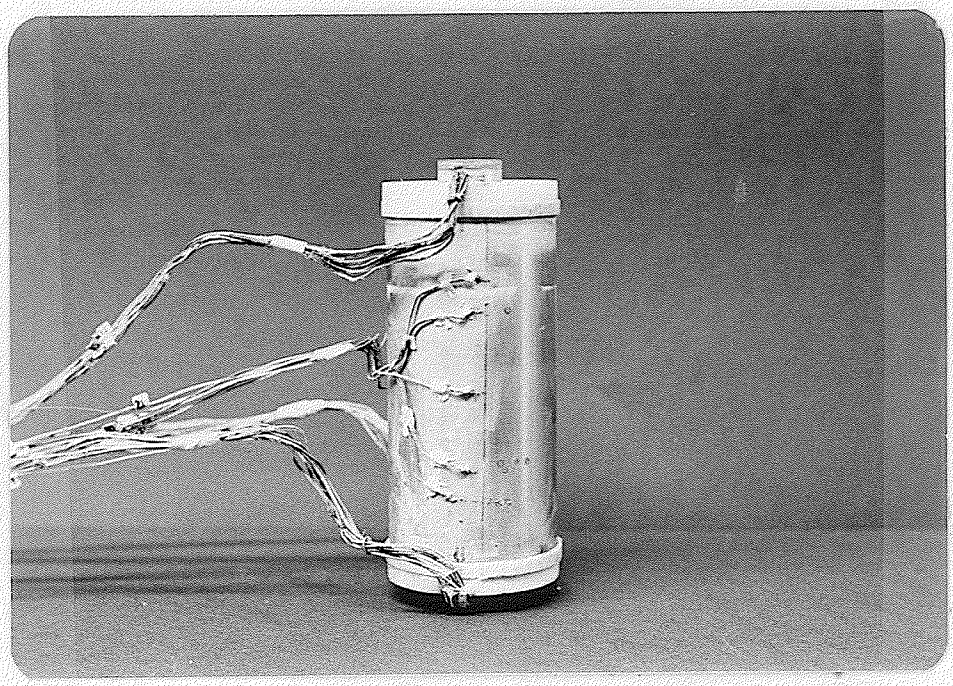

Fig. 28 Test Specimen TCR-2 Showing Spot-Welded Thermocouples

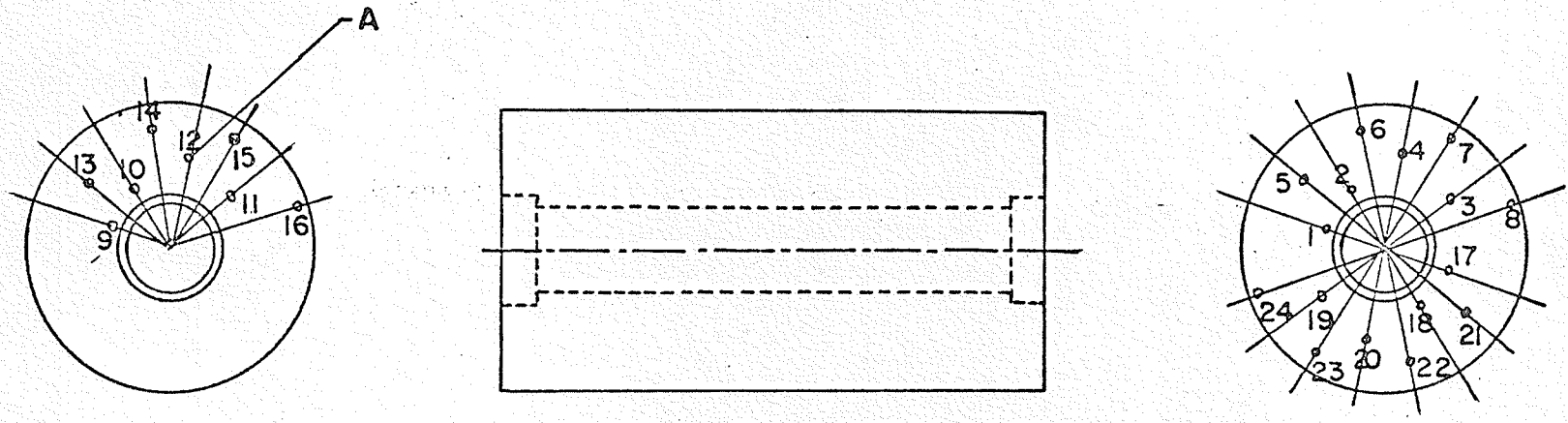

Legend : A — 0.040 in. dia. drilled hole

Radial Dist. (in.)	0.594	0.714	0.834	0.954	1.074	1.22	1.30	1.37	
Upper Level	1	2	3	4	5	6	7	8	— 1.50 in. deep
Lower Level	9	10	11	12	13	14	15	16	— 2.86 in. deep
Mid Level	17	18	19	20	21	22	23	24	— 1.50 in. deep

Fig. 29 Location of Thermocouple Wells for Specimen TCR-2

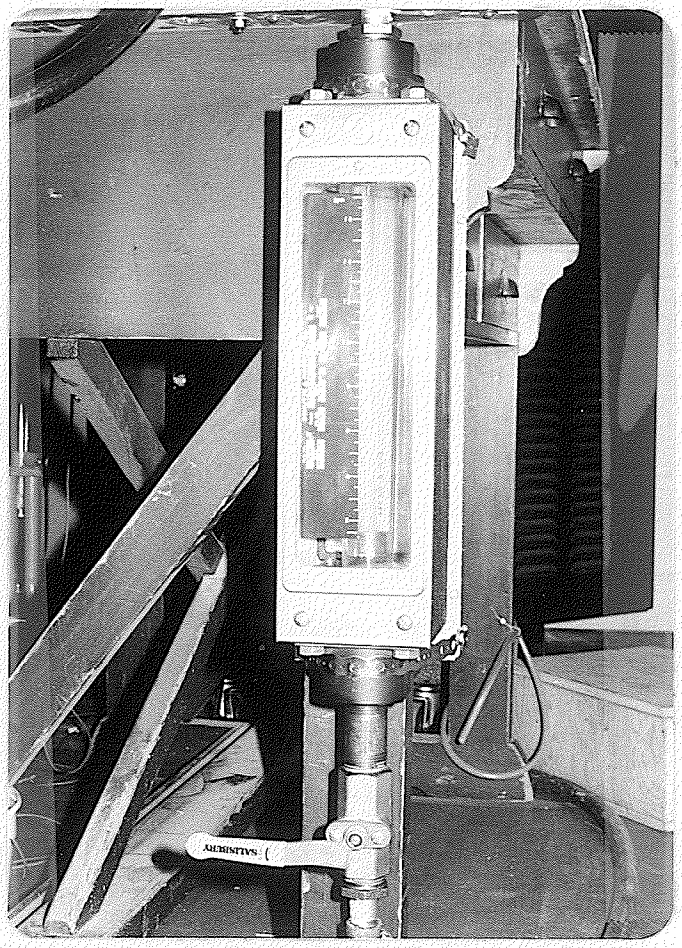

Fig. 30 Schattle & Koerting Water Flow Meter

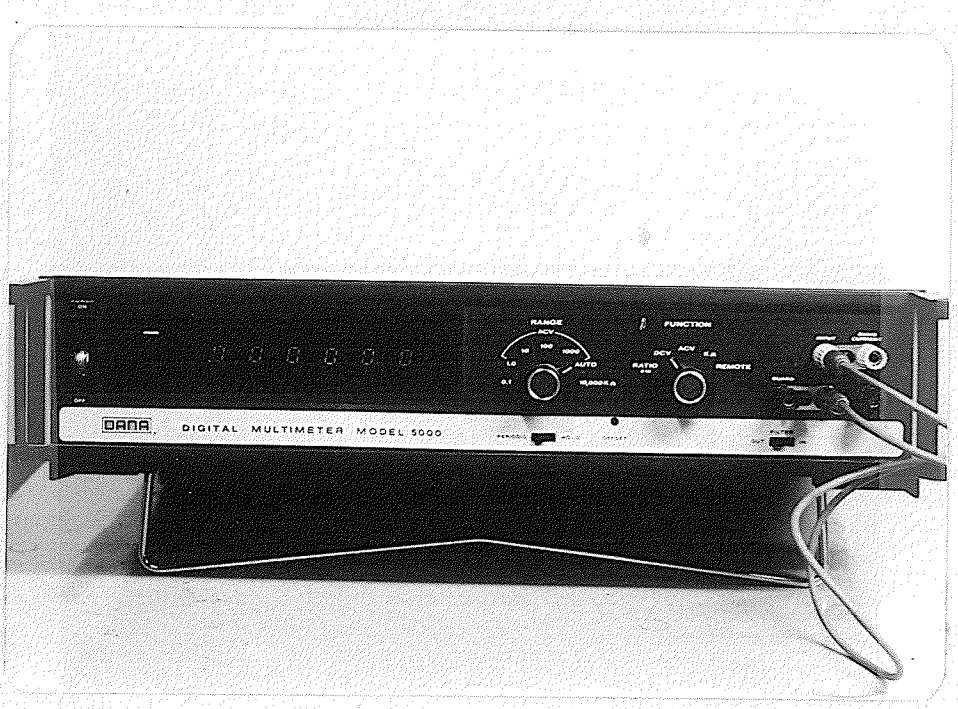

Fig. 31 DANA Digital Multimeter

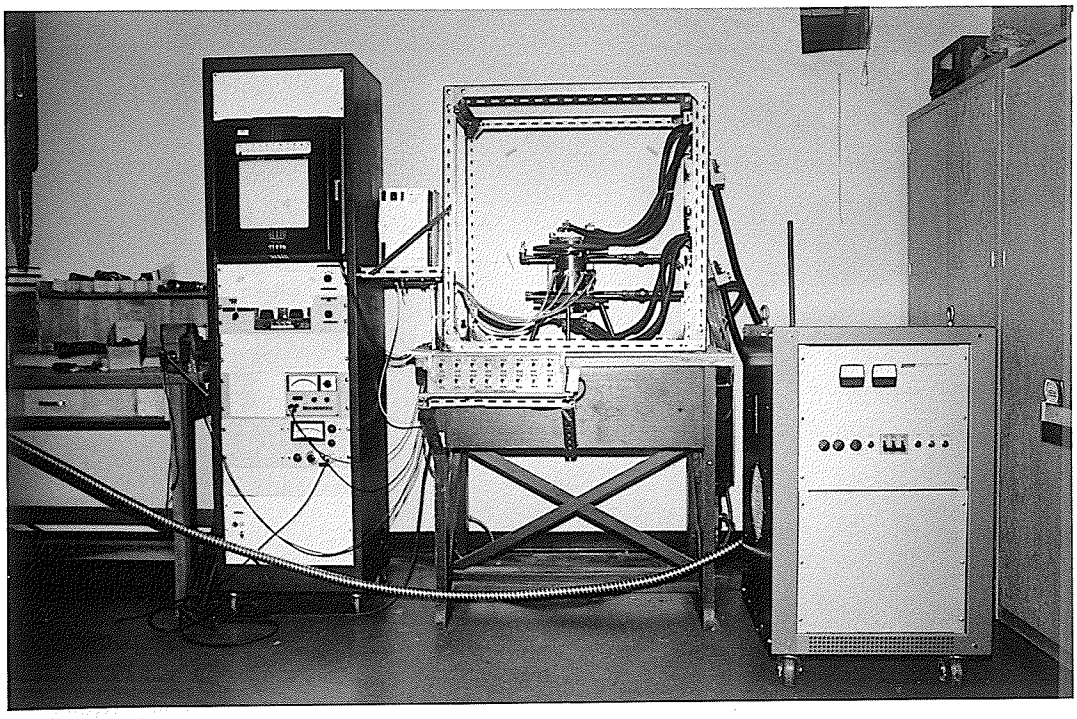

Fig. 32 Arrangement of Test Equipment

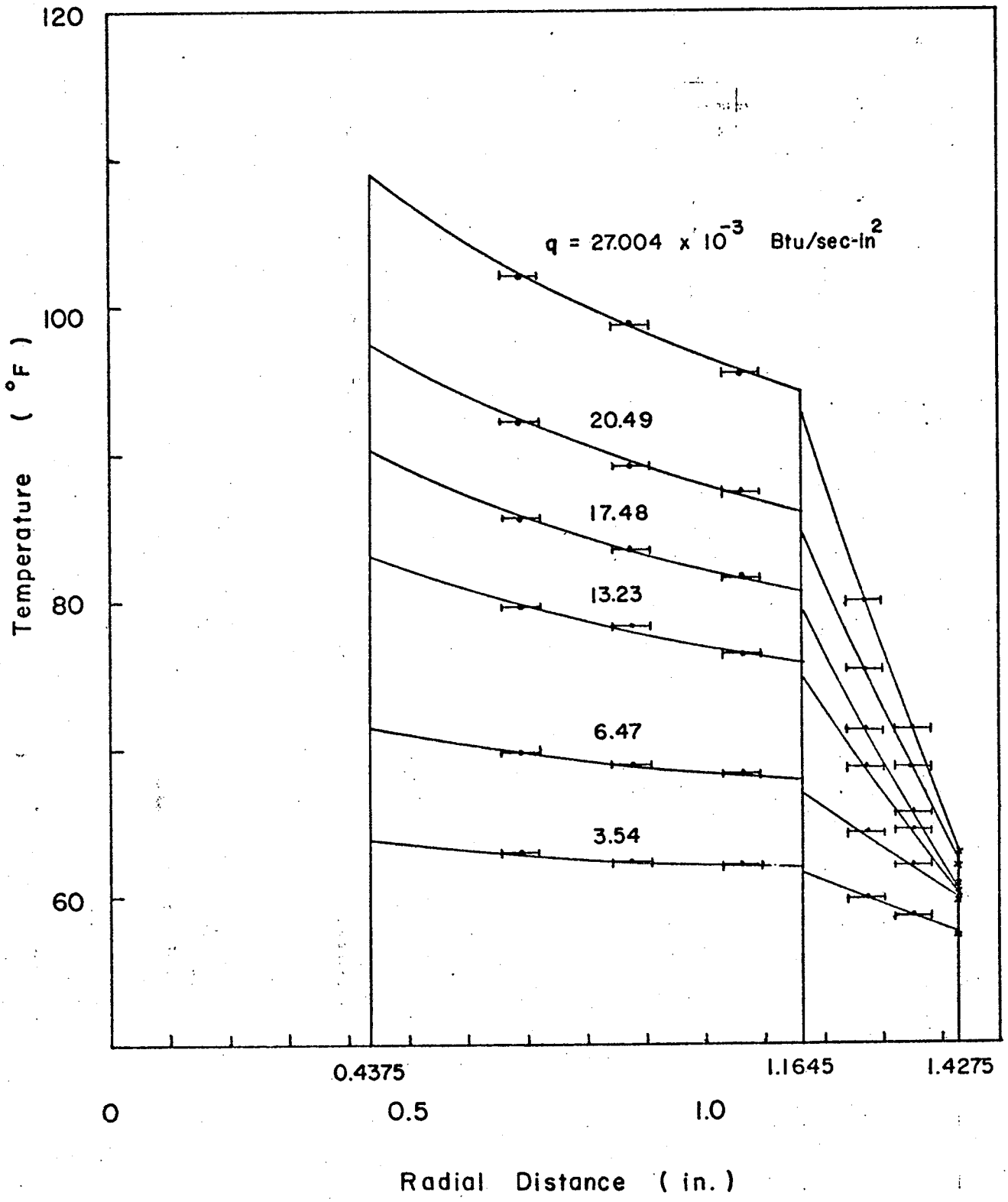

Fig. 33 Temperature Distribution for TCR-1

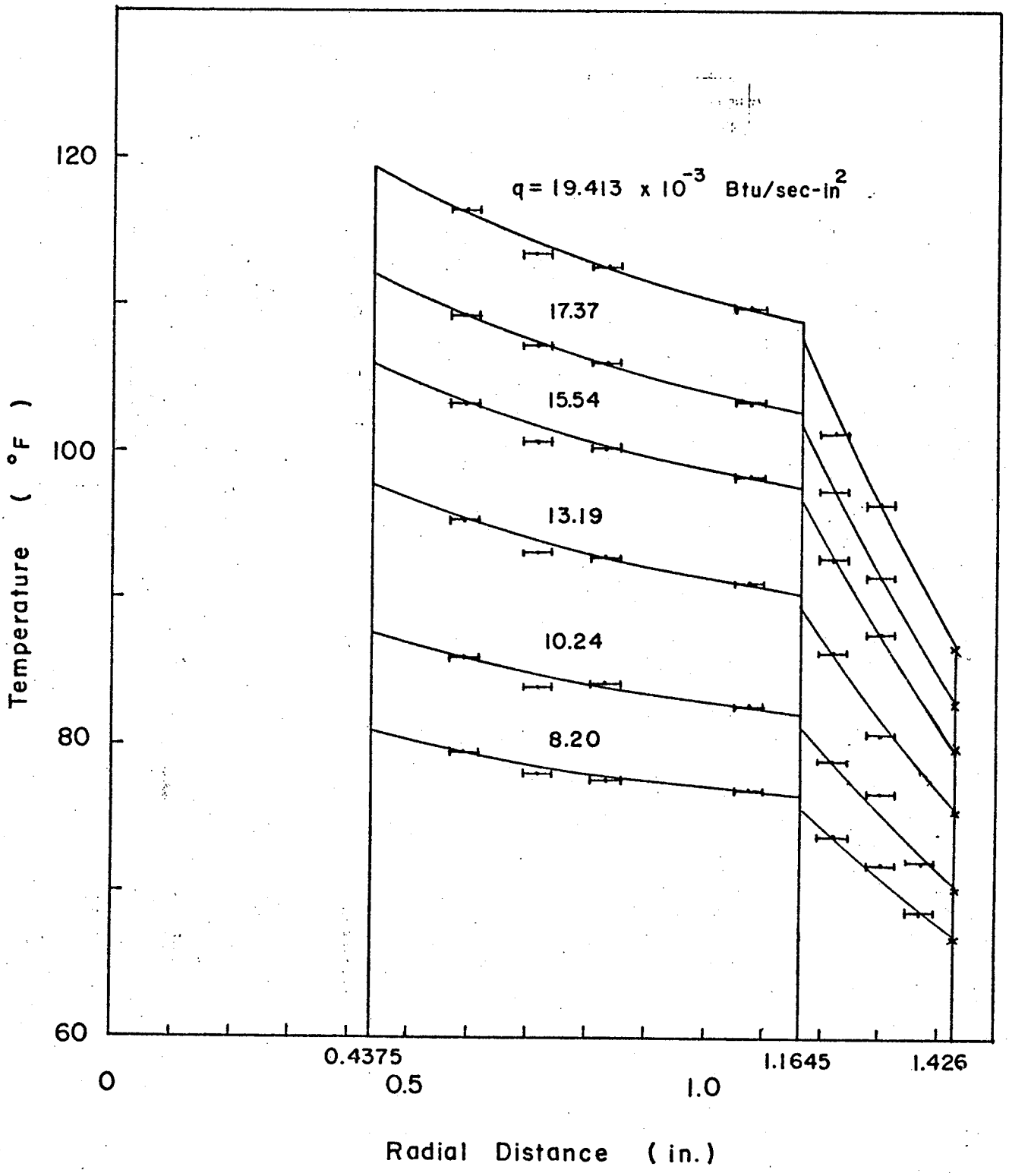

Fig. 34 Temperature Distribution for TCR-2

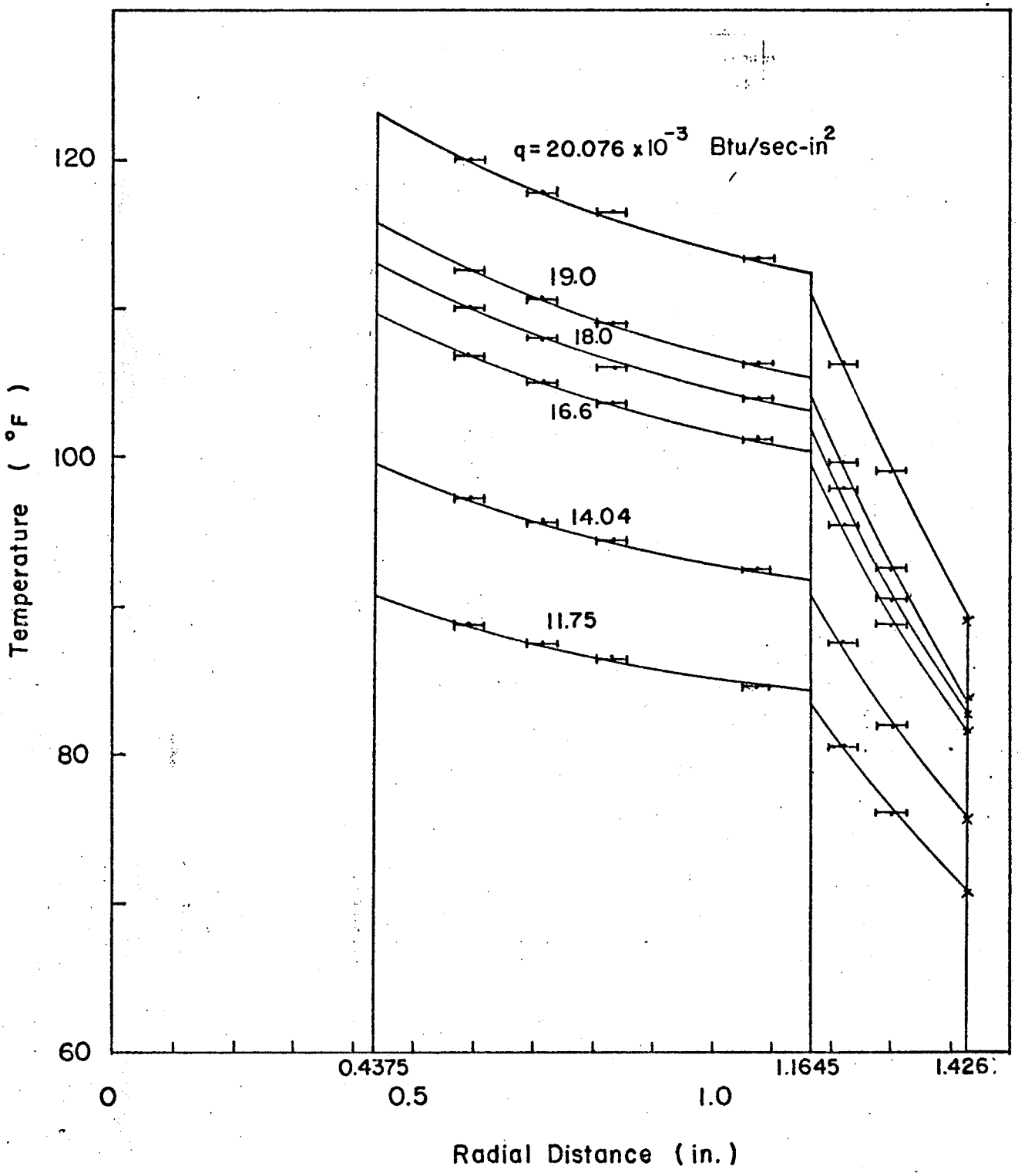

Fig. 35 Temperature Distribution For TCR-2.XR

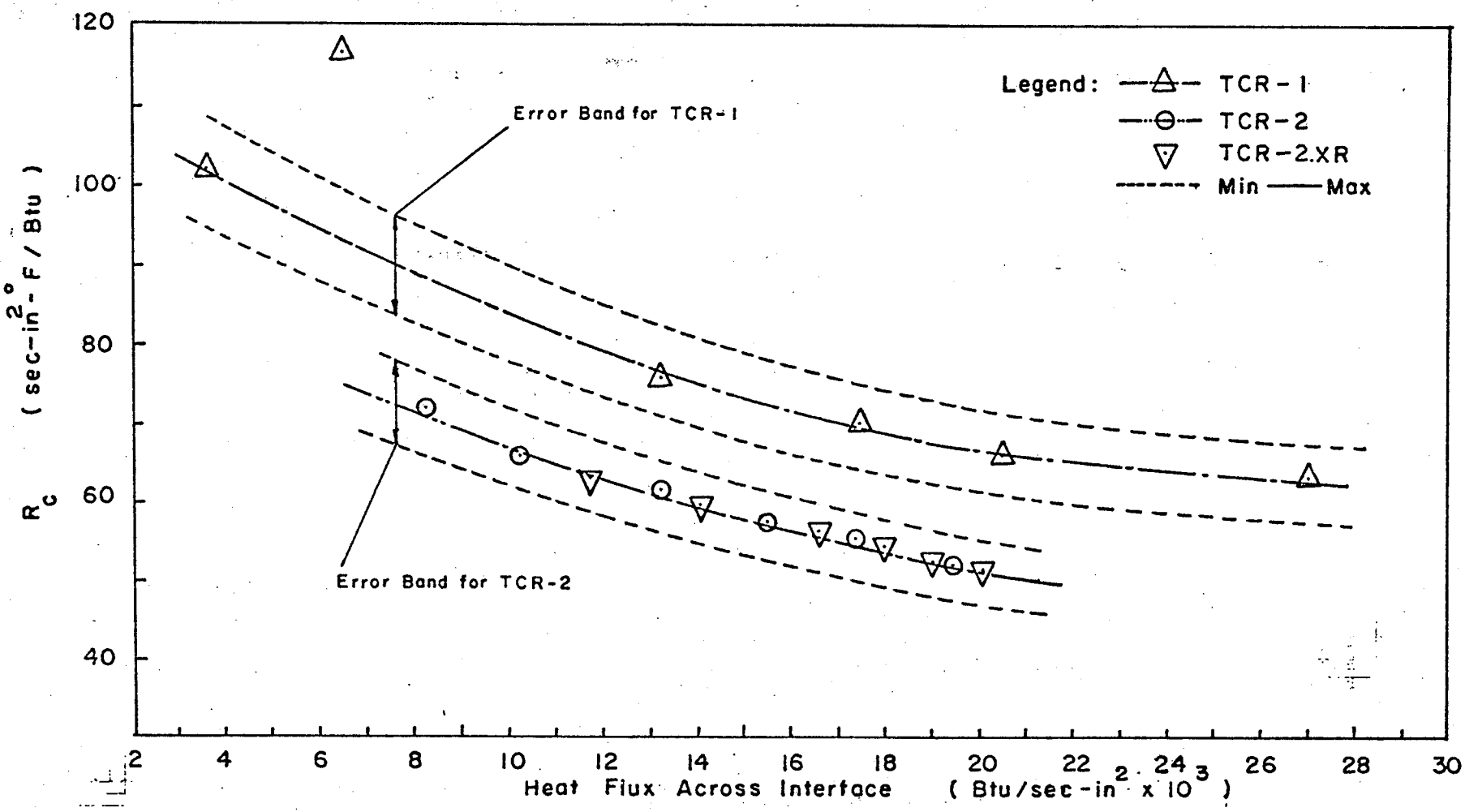

Fig. 36 Thermal Contact Resistance vs Heat Flux Across Interface

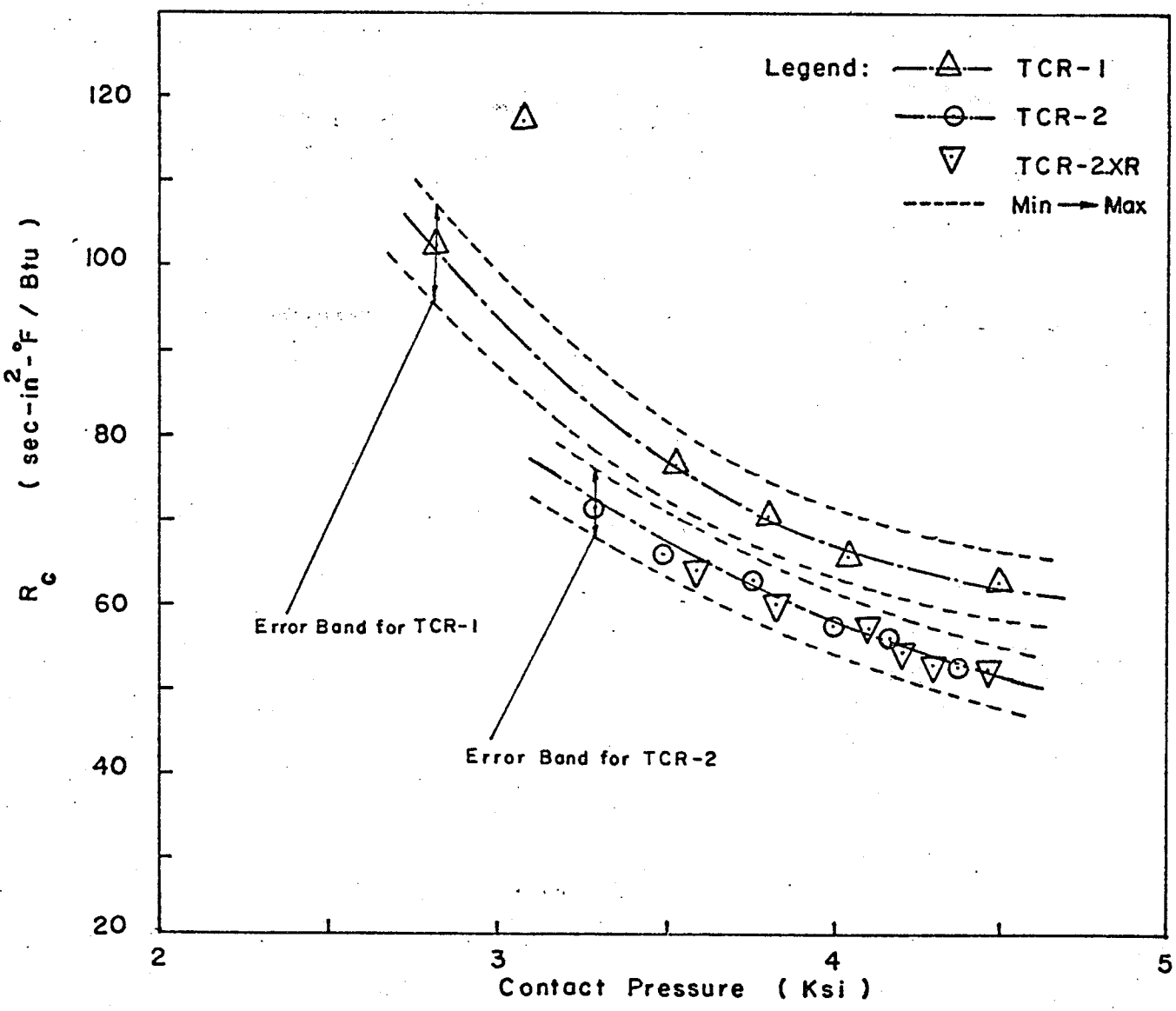

Fig. 37 Thermal Contact Resistance vs Contact Pressure

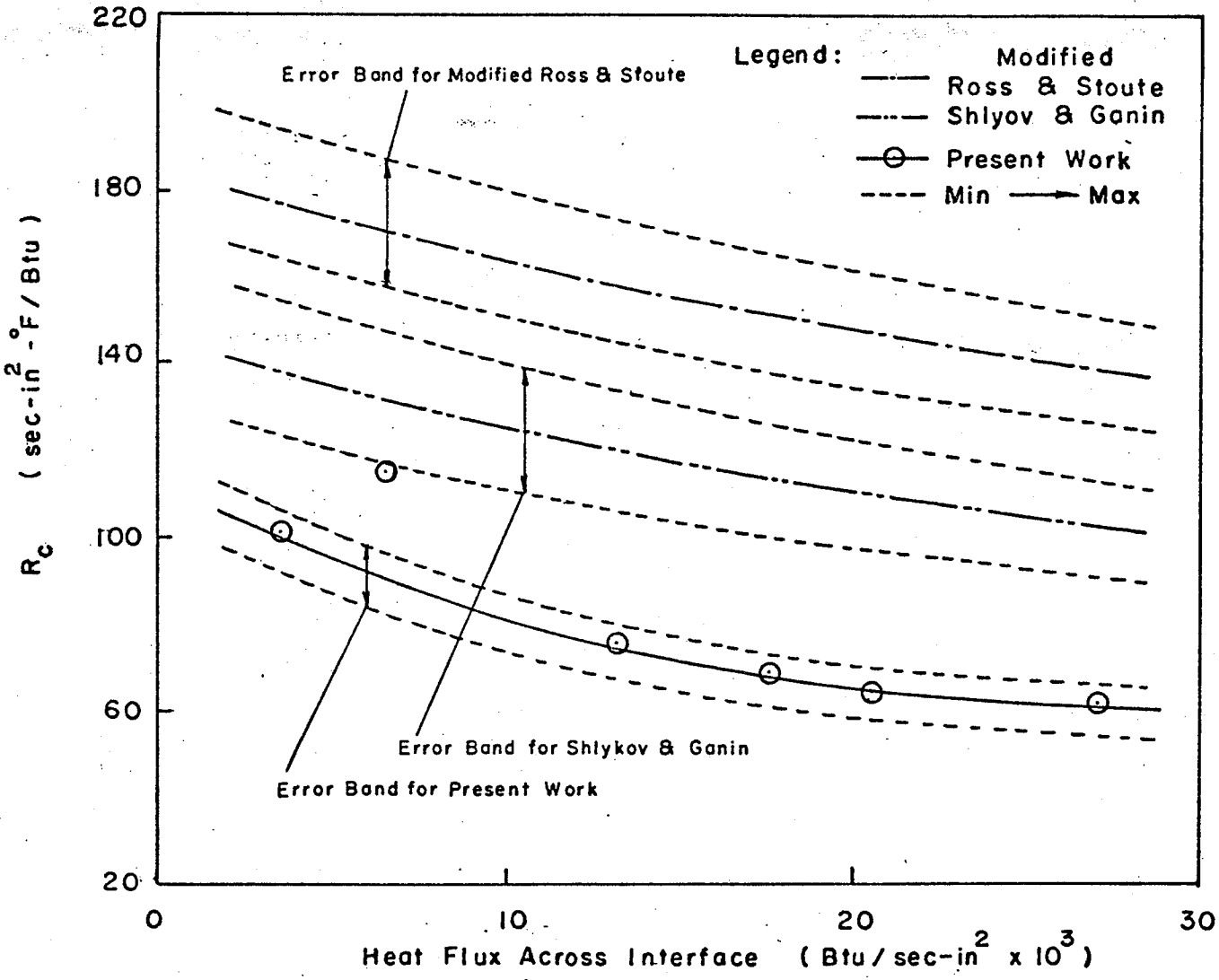

Fig. 38 Thermal Contact Resistance vs Heat Flux Across Interface for TCR-1

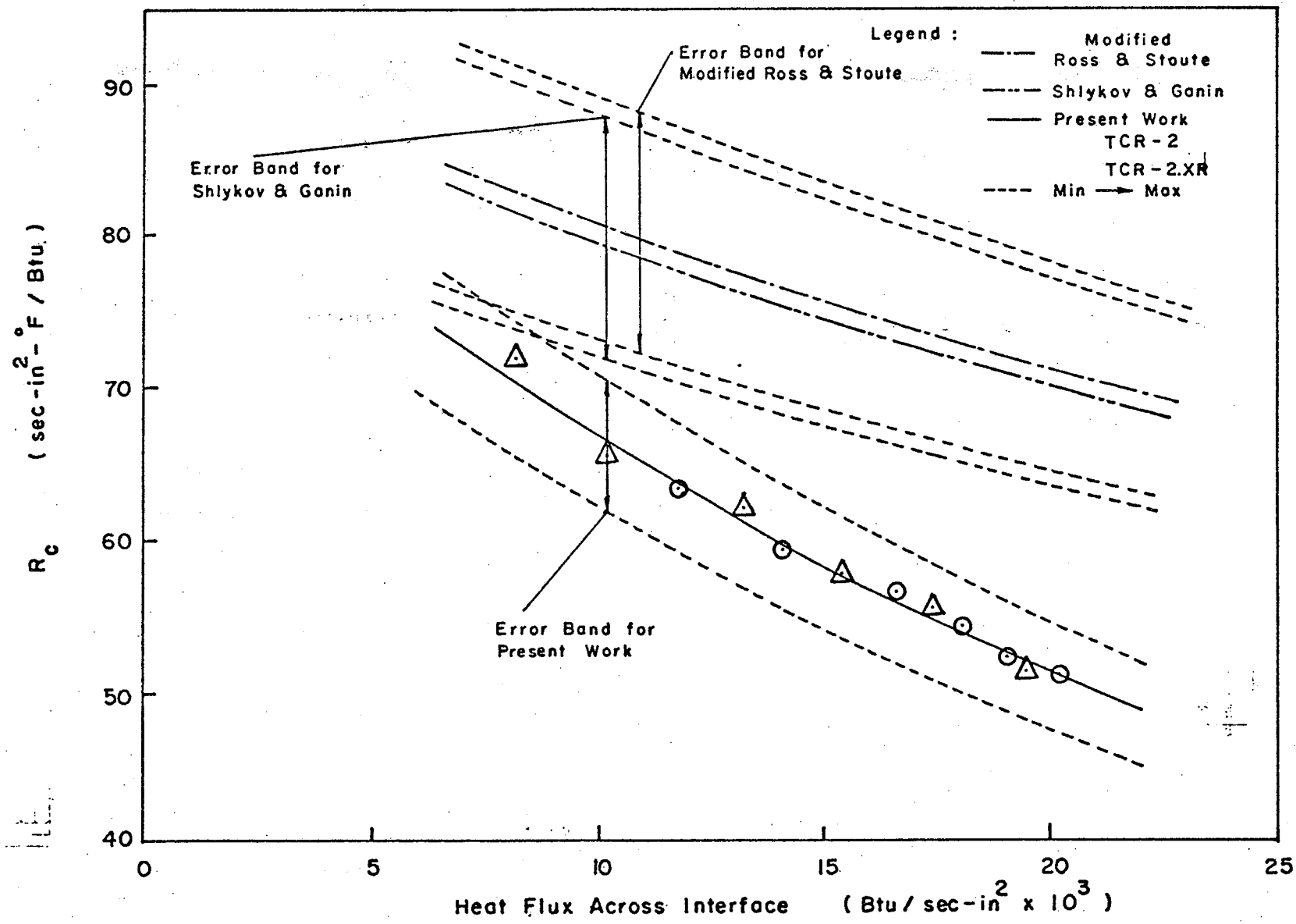

Fig. 39 Thermal Contact Resistance vs Heat Flux Across Interface for TCR-2

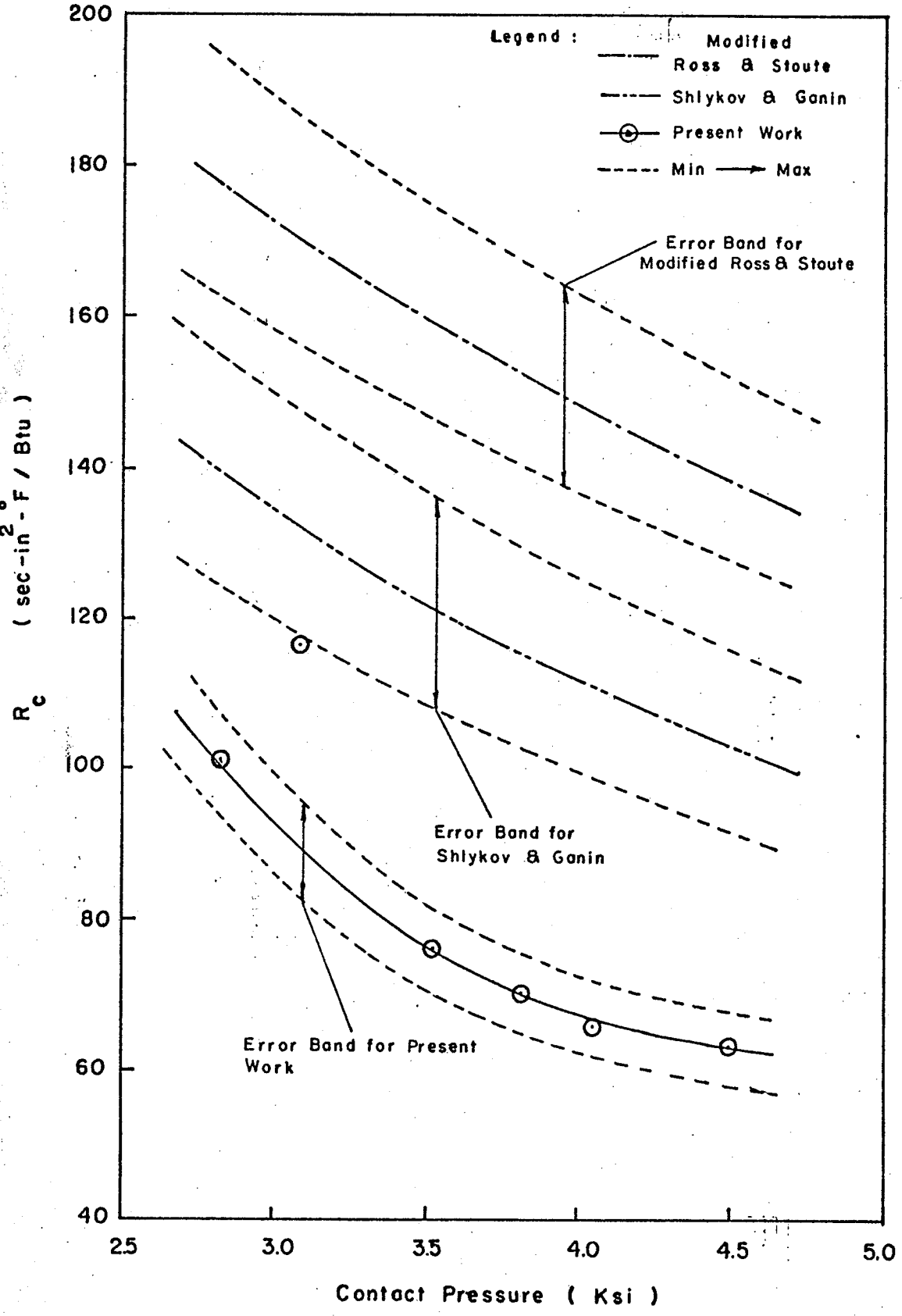

Fig. 40 Thermal Contact Resistance for TCR-1

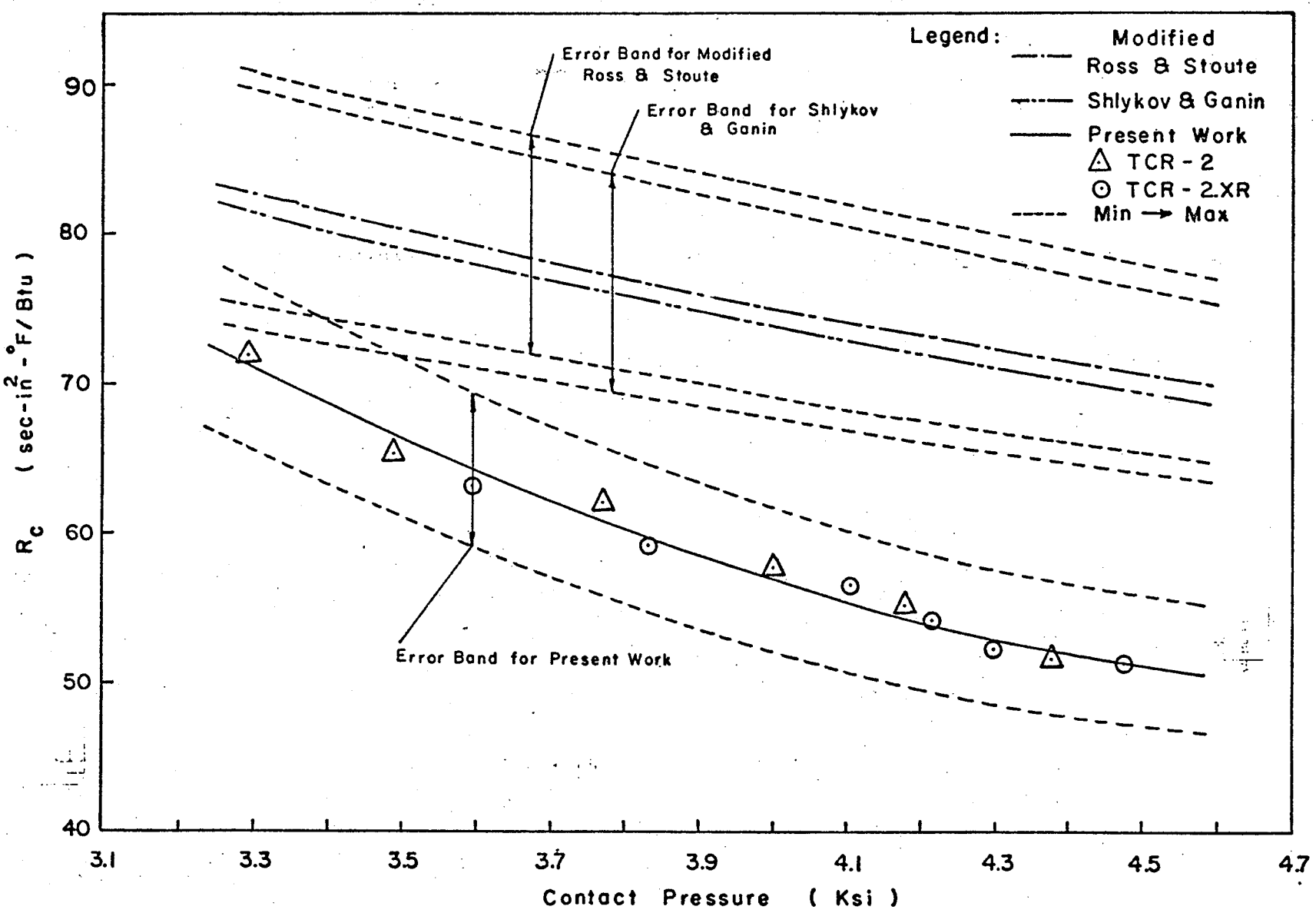

Fig. 41 Thermal Contact Resistance for Specimen TCR-2

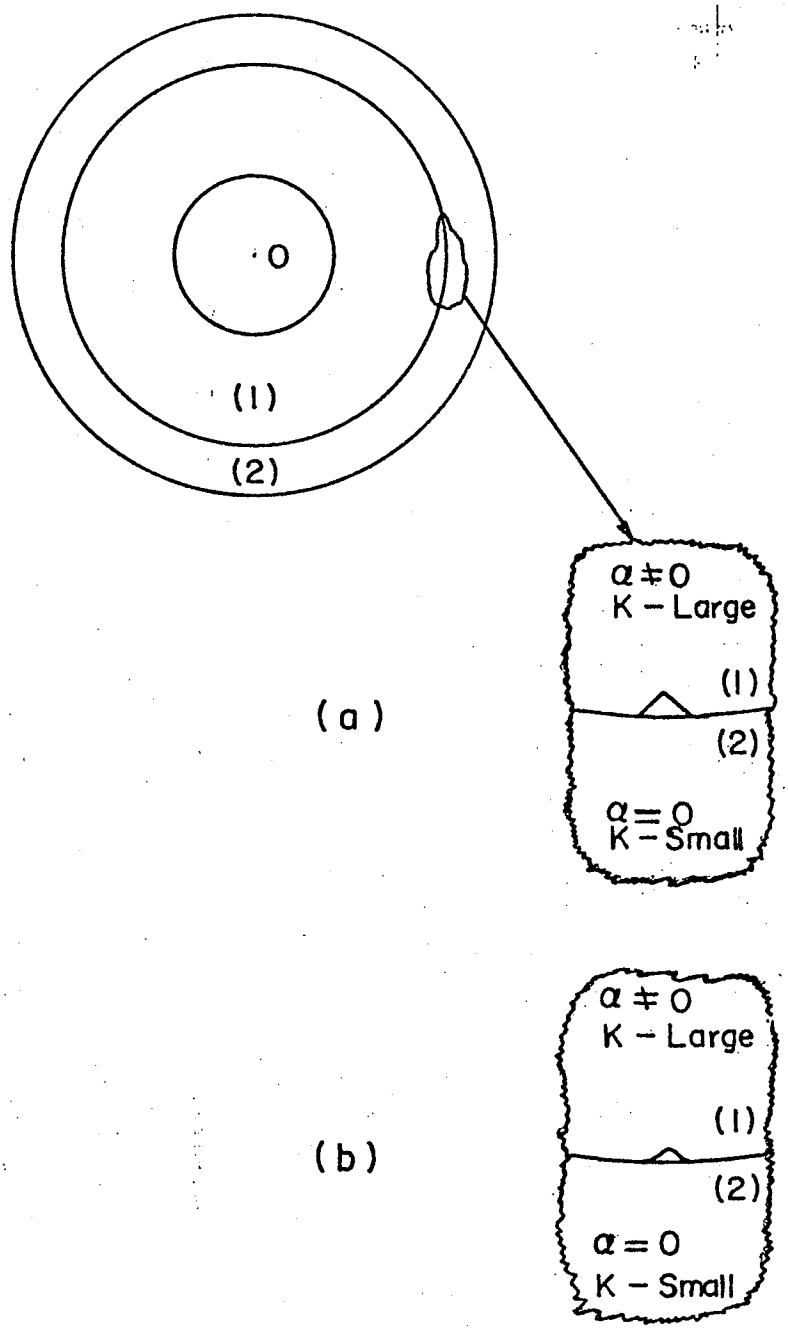

Fig. 42 Physical Interface Model with Discontinuity in Material of High Thermal Conductivity:
(a) Initial Geometry;
(b) Geometry for Heat Flow from (1) to (2).

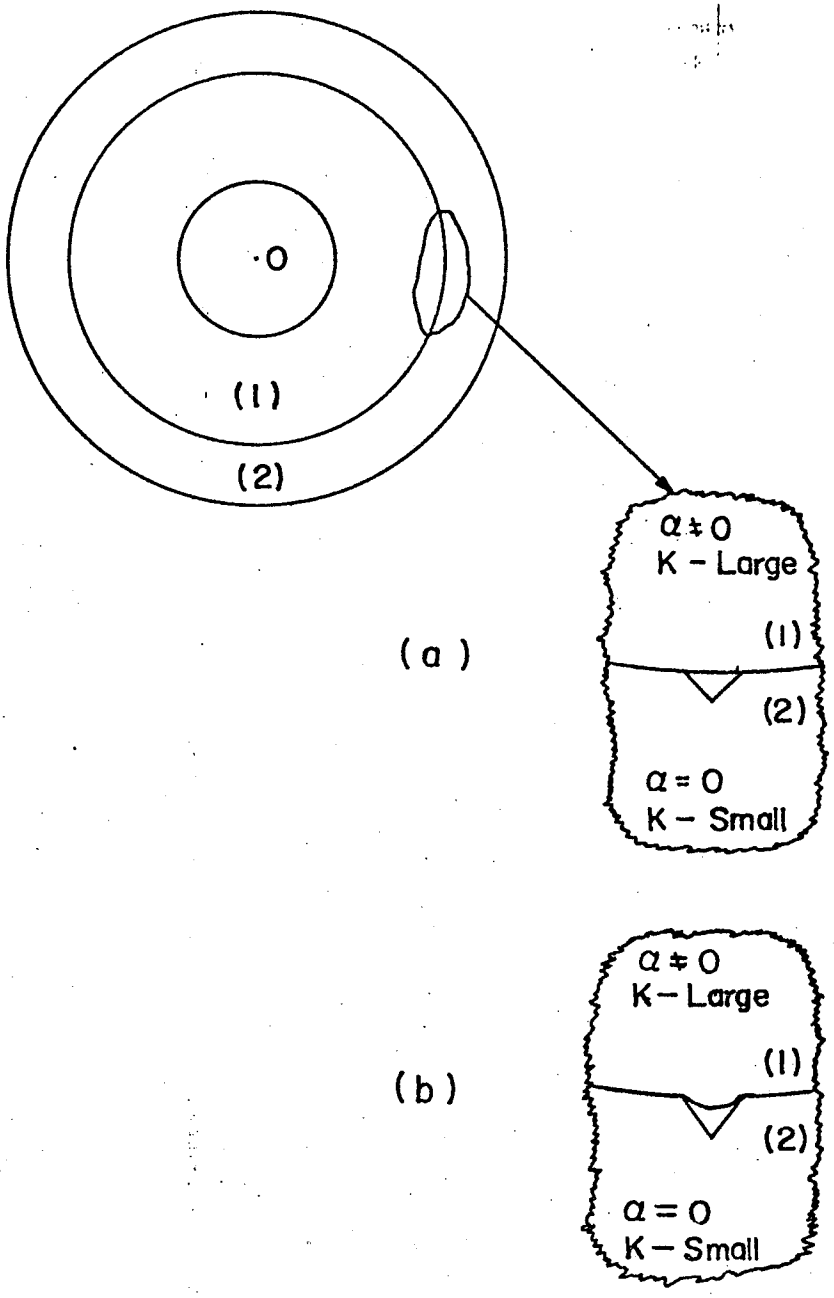

Fig. 43 Physical Interface Model with Discontinuity in Material of Low Thermal Conductivity:
(a) Initial Geometry;
(b) Geometry for Heat Flow from (1) to (2).

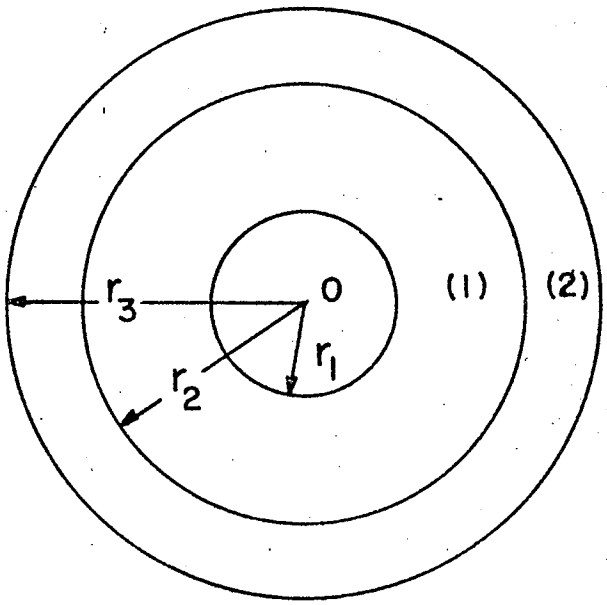

Fig. 44 Sketch of Compound Cylinder